

PREPARATION AND CHARACTERIZATION OF MICRON SIZE  
SERPENTINE FILLED ABS COMPOSITE

A THESIS SUBMITTED TO  
THE GRADUATE SCHOOL OF NATURAL AND APPLIED SCIENCES  
OF  
MIDDLE EAST TECHNICAL UNIVERSITY

BY

MUSTAFA CAN ALAKOÇ

IN PARTIAL FULFILLMENT OF THE REQUIREMENTS  
FOR  
THE DEGREE OF MASTER OF SCIENCE  
IN  
POLYMER SCIENCE AND TECHNOLOGY

NOVEMBER 2008

Approval of the thesis:

**PREPARATION AND CHARACTERIZATION OF MICRON SIZE  
SERPENTINE FILLED ABS COMPOSITE**

submitted by **MUSTAFA CAN ALAKOÇ** in partial fulfillment of the requirements  
for the degree of **Master of Sciences in Polymer Science and Technology**  
**Department, Middle East Technical University** by,

Prof. Dr. Canan Özgen  
Dean, Graduate School of **Natural and Applied Sciences**

\_\_\_\_\_

Prof. Dr. Cevdet Kaynak  
Head of Department, **Polymer Science and Technology**

\_\_\_\_\_

Prof. Dr. Teoman Tinçer  
Supervisor, **Chemistry Dept., METU**

\_\_\_\_\_

Assoc. Prof. Dr. Göknur Bayram  
Co-Supervisor, **Chemical Engineering Dept., METU**

\_\_\_\_\_

**Examining Committee Members:**

Prof. Dr. Leyla Aras  
Chemistry Dept., METU

\_\_\_\_\_

Prof. Dr. Teoman Tinçer  
Chemistry Dept., METU

\_\_\_\_\_

Assoc. Prof. Dr. Göknur Bayram  
Chemical Engineering Dept., METU

\_\_\_\_\_

Prof. Dr. Ali Usanmaz  
Chemistry Dept., METU

\_\_\_\_\_

Prof Dr. Mehmet Saçak  
Chemistry Dept., Ankara University

\_\_\_\_\_

**Date:** 27.11.2008

**I hereby declare that all information in this document has been obtained and presented in accordance with academic rules and ethical conduct. I also declare that, as required by these rules and conduct, I have fully cited and referenced all material and results that are not original to this work.**

Name, Last Name : Mustafa Can ALAKOÇ

Signature :

## ABSTRACT

### PREPARATION AND CHARACTERIZATION OF MICRON SIZE SERPENTINE FILLED ABS COMPOSITE

Alakoç, Mustafa Can

M.S., Department of Polymer Science and Technology

Supervisor: Prof. Dr. Teoman Tinçer

Co-Supervisor: Assoc. Prof. Dr. Göknur Bayram

November 2008, 64 pages

Micron size non-treated / silane coupling agent (SCA) treated serpentine filled acrylonitrile-butadiene-styrene (ABS) composite preparation and characterization of composites in terms of mechanical, thermal, flow properties and morphology were studied in this work. First step of the study was the size reduction of the as collected serpentine mineral. Secondly, three types of silane coupling agent treatments were applied to serpentine which were  $\gamma$ -methacryloxypropyltrimethoxysilane (A-174),  $\beta$ -(3,4-epoxycyclohexyl)-ethyltrimethoxysilane (A-186) and  $\gamma$ -mercapto-propyltrimethoxysilane (A-189). Non-treated and three different types of SCA treated serpentine minerals were melt mixed with ABS. Non-treated serpentine filled ABS composites had the serpentine weight fractions of 2%, 5%, 10% and 20%. On the other hand, SCA treated ones had serpentine weight fractions of 2%, 5% and 10%.

Morphological analysis showed that SCA treatment was partly effective in interface interaction enhancement and A-186 gave the best results according to micrographs. There wasn't any critical mechanical property loss up to 20% serpentine addition.

Tensile tests revealed that SCA treatment increased the yield strength values of composites compared to non-treated serpentine filled composites. In accordance with morphological study, best result was obtained from 5% A-186 treated serpentine filled ABS as 12.9% improvement in yield strength value. Percent elongation at break values were increased with filler addition and greatest increase was observed in A-189 treated samples. Serpentine addition had no net effect on Young's Modulus values. According to the impact testing results, A-189 treated samples had improved toughness compared to non-treated samples in accordance with elongation at break values. However increasing filler content resulted with decrease in impact strength values. DSC analysis showed that glass transition temperatures, especially for SCA treated samples, were decreased compared to neat ABS with filler addition. This result suggests that SCA may had the plasticizing effect on the composite. Flow properties of composites were not different from neat ABS up to 2% addition, when the filler concentration was further increased melt flow index values were dramatically decreased.

Keywords: Serpentine, ABS/Serpentine Composite, Filler, Silane Coupling Agent

## ÖZ

### MİKRON BOYUTLU SERPENTİN KATKILI ABS KOMPOZİTİNİN HAZIRLANIŞI VE KARATERİZASYONU

Alakoç, Mustafa Can

Yüksek Lisans, Polimer Bilimi ve Teknolojisi

Tez Yöneticisi: Prof. Dr. Teoman Tinçer

Ortak Tez Yöneticisi: Doç. Dr. Gökür Bayram

Kasım 2008, 64 sayfa

Bu çalışmada mikron boyutlu işlem uygulanmamış/silan bağlayıcılar(SCA) uygulanmış serpentin içeren akrilonitril butadien stiren kompozitlerinin hazırlanışı ve bu kompozitlerin mekanik, ısıl, akışkanlık özellikleri ile morfolojileri çalışılmıştır. Çalışmanın ilk basamağında, toplanmış olan serpentin mineralinin boyut küçültme işlemi yapılmıştır. İkinci olarak  $\gamma$ -metakriloksi propil trimetoksisilan(A-174),  $\beta$ -(3,4-epoksisikloheksil)-etil trimetoksisilan (A-186) ve  $\gamma$ -merkaptopropil trimetoksisilan (A-189) silan bağlayıcıları serpentine uygulanmıştır. İşlem uygulanmamış ve silan bağlayıcı uygulanmış serpentin/ABS kompozitleri, eriyik karıştırma yöntemiyle hazırlanmıştır. İşlem uygulanmamış serpentinle hazırlanan kompozitlerin ağırlıkça serpentin oranları 2%, 5%, 10% ve 20%'dir. Silan bağlayıcı uygulanan kompozitler ağırlıkça 2%, 5% ve 10% serpentin içermektedirler.

Morfolojik analiz göstermiştir ki silan bağlayıcı uygulaması, arayüzeydeki etkileşimin geliştirilmesini kısmen sağlamıştır ve mikrograflara göre en iyi sonuç A-186 silan bağlayıcısıyla elde edilmiştir. 20% serpentin içeriğine kadar mekanik özelliklerde kritik bir kayıp yaşanmamıştır. Gerilme testleri, serpentin silan bağlayıcı

uygulamasý yapılan kompozitlerin çekme gerilme dayanýmlarýnÝn, iŖlem uygulanmayan serpentin eklenen kompozitlere göre daha yüksek olduđunu ortaya çýkarmýŖtır. Morfolojik çalıŖmalara uygun olarak 5% serpentin ieren kompozitte maksimum çekme gerilmesi deđeri 12.9% artýŖ göstererek en büyük geliŖimi sergilemiŖtir. Kopmada yüzde uzama deđerleri serpentin eklenmesiyle birlikte artýŖ göstermiŖtir ve en fazla artýŖ A-189 uygulanan kompozitlerde görülmüŖtür. Serpentin eklenmesinin elastik modüline belirgin bir etkisi saptanmamýŖtır. Darbe dayanımı testlerinin sonuçlarına göre, kopmada uzama sonuçlarıyla uyumlu bir Ŗekilde, A-189 uygulanan kompozitlerin tokluđu, katkısýz ABS'ye göre artmýŖtır. Ancak, kompozitin iindeki katkı maddesi arttırıldıđında toklukta düŖüŖ gözlemlenmiŖtir. DSC analizi, özellikle silan uygulamasý yapılan kompozitlerde, serpentin eklenmesiyle birlikte kompozitlerin camsý geiŖ sıcaklıđının, ABS'nin camsý geiŖ sıcaklıđına göre düŖtüđünü göstermiŖtir. Bu sonuçla birlikte silan uygulamasýnÝn kompozitler üzerinde plastikleŖtirici etki göstermiŖ olabileceđi anlaŖılmýŖtır. 2% serpentin eklenmesine kadar kompozitlerin akýŖ özellikleri ABS'ye göre farklılık göstermemiŖtir ancak daha yüksek serpentin eklenmesi durumunda kompozitlerin eriyik akýŖ indisi dramatik bir biçimde azalmýŖtır.

Anahtar Kelimeler: Serpentin, ABS/Serpentin Kompoziti, Katkı Maddesi, Silan Bađlayıcı

To my family and to Ezgi

## ACKNOWLEDGEMENT

I would like to express my deepest gratitude to my thesis supervisor Prof. Dr. Teoman Tinçer for his guidance, understanding, kind support, encouraging advices, criticism, and valuable discussions throughout my thesis. I am greatly indebted to my thesis co-supervisor Assoc. Prof. Dr. Göknur Bayram from Department of Chemical Engineering for her regardful guidance during formation of this dissertation and for providing me every opportunity to use the instruments in her laboratory, Prof. Dr. Erdal Bayramlı from Department of Chemistry for his permission to use the injection molding machine in his laboratory.

Special thanks go to from Sevim Ulupınar Chemistry Department for DSC analysis, Cengiz Tan from Metallurgical and Materials Engineering Department for SEM analysis and Osman Yaslıtaş from Chemistry Department.

I express my special thanks to Semra Can for sparing her time and her all help during my experiments. I would also like to thank to my friends Tuğba Efe, Şafak Kaya, Binnur Özkan, Gökhan Yılmaz for cooperation and friendship, and helping me in all the possible ways.

It is with immense pleasure that I dedicate this dissertation to my family, Ayhan, Ali and Ceren who always offered their advice, love, care and support. My family's absolute unquestionable belief in me have been a constant source of encouragement and have helped me achieving my goals. I also express my deepest love and thanks to Ezgi Erdoğan for her love, patience, support, understanding and encouragement in every step of this study. This process would be nothing but an eczema initiator if I couldn't feel her love and support each and every minute.

## TABLE OF CONTENTS

ABSTRACT .....	iv
ÖZ .....	vi
DEDICATION.....	vii
ACKNOWLEDGEMENT .....	ix
TABLE OF CONTENTS .....	x
LIST OF TABLES.....	xii
LIST OF FIGURES .....	xiii
CHAPTERS	
1. INTRODUCTION .....	1
1.1 Composite Materials.....	1
1.2 Composite Materials Using Polymers as Matrix .....	2
1.2.1 Particulate Composites with Polymer Matrix .....	3
1.2.1.1 Mineral Fillers .....	4
1.2.1.2 Synthetic Particulate Fillers .....	5
1.3 Layered Silicate Minerals .....	5
1.3.1 Serpentine.....	7
1.4 Silane Coupling Agents .....	8
1.4.1 Silane Coupling Agents & Fillers.....	9
1.4.2 Types of Silane Coupling Agents.....	10
1.4.2.1 Vinylsilanes .....	10
1.4.2.2 Methacryloxysilanes .....	11
1.4.2.3 Epoxysilanes.....	11
1.4.2.4 Aminosilanes .....	11
1.4.2.5 Sulfur Functional Silanes .....	11
1.5 Acrylonitrile – Butadiene – Styrene (ABS).....	12
1.5.1 Special Grades of ABS .....	14
1.5.2.1 ABS – Filler Composite Studies.....	15
1.5.2.2 ABS – Clay Composite Studies.....	17

1.6	Aim of the Study .....	19
2.	EXPERIMENTAL.....	20
2.1	Materials .....	20
2.1.1	ABS.....	20
2.1.2	Serpentine .....	21
2.1.3	Silane Coupling Agents .....	21
2.2	Experimental Procedure .....	23
2.2.1	Size Reduction of Serpentine.....	23
2.2.2	Silane Coupling Agent Treatment.....	23
2.2.3	Melt Mixing by Extrusion.....	24
2.2.4	Injection Molding .....	25
2.3	Sample Characterization.....	26
2.3.1	Tensile Testing.....	26
2.3.2	Impact Testing.....	27
2.3.3	DSC .....	27
2.3.4	MFI.....	27
2.3.5	SEM.....	27
3.	RESULTS AND DISCUSSION.....	28
3.1	Morphological Characterization .....	28
3.1.1	Scanning Electron Microscopy Analysis.....	28
3.2.	Mechanical Analysis .....	42
3.2.1.	Tensile Testing .....	42
3.2.1.1	Yield Strength and Elongation at Break .....	42
3.2.1.2	Young's Modulus .....	47
3.2.2	Impact Testing.....	50
3.3.	Thermal Characterization by DSC Analysis .....	51
3.4.	Flow Characteristics Determination by Melt Flow Index (MFI) Analysis .....	52
4.	CONCLUSIONS .....	54
	REFERENCES .....	56
	APPENDICES	
A.	TENSILE PROPERTIES DATA.....	60
B.	DSC THERMOGRAMS .....	62

## LIST OF TABLES

### TABLES

Table 2. 1 Some properties of ABS .....	20
Table 2. 2 Properties of SCAs .....	22
Table 2. 3 Final value of average particle size of serpentine powder after size reduction process .....	23
Table 2. 4 Extrusion process variables .....	24
Table 2. 5 Prepared ABS-Serpentine Composites, compositions and SCA contributions .....	25
Table 2. 6 Dimensions of dumbbell specimen .....	26
Table 3. 1 $T_g$ values derived from DSC thermograms.....	52
Table 3. 2 MFI results of all samples.....	52
Table A. 1 Average Yield Strength and Percent Elongation at Break Values for Composites.....	60
Table A. 2 Young's Modulus Values for Composites.....	61
Table A. 3 Impact Strength Values for Composites .....	61

## LIST OF FIGURES

### FIGURES

Figure 1.1 A single tetrahedral (up side left), a sheet structure of silica tetrahedral arranged in a hexagonal network (up side right), a single octahedral unit (down side left) and a sheet structure of octahedral units (down side right).....	6
Figure 1.2 (a) 1:1 – Kaolinite - $\text{Al}_4\text{Si}_4\text{O}_{20}(\text{OH})_8$ (b) 2:1 – Montmorillonite - $\text{Al}_4(\text{Si}_4\text{O}_{10})_2(\text{OH})_8 \cdot x\text{H}_2\text{O}$ (c) 2:1:1 – Chlorite – $\text{Mg}_{10}\text{Al}_2(\text{Si}_6\text{Al}_2)\text{O}_{20}(\text{OH})_{16}$ .....	7
Figure 1.3 General structure of organosilanes.....	9
Figure 1.4 Mode of reaction between a silanol and an inorganic surface.....	9
Figure 1.5 Overview of a silanized surface.....	10
Figure 1.6 Grafting reaction of butadiene onto SAN.....	13
Figure 1.7 Chemical steps involved in the preparation of ABS .....	14
Figure 2.1 Chemical Structures of (a) A-174 (b) A-186 and (c) A-189 .....	22
Figure 2.2 Representation of a dumbbell shaped specimen.....	26
Figure 3.1 SEM image of fractured surface of ABS-5 (a) x2000–1 (b) x2000–2 .....	30
Figure 3.2 SEM image of fractured surface of ABS-10 (a) x500 (b) x3000 .....	31
Figure 3.3 SEM image of fractured surface of ABS-20 (a) x2000 (b) x25227.....	32
Figure 3.4 SEM image of fractured surface of ABS-2-174 (a) x1000 (b) x2000 ....	33
Figure 3.5 SEM image of fractured surface of ABS-5-174 (a) x1000-1 (b) x1000-2 .....	34
Figure 3.6 SEM image of fractured surface of ABS-10-174 (a) x1000–1 (b) x1000–2 .....	35
Figure 3.7 SEM image of fractured surface of ABS-2-186 (a) x500x (b) x20000 ...	36
Figure 3.8 SEM image of fractured surface of ABS-5-186 (a)x2000 (b)x10000 (c)x20000 .....	38

Figure 3. 9 SEM image of fractured surface of ABS-10-186 (a)x2000-1 (b)x2000-2 .....	39
Figure 3. 10 SEM image of fractured surface of ABS-5-189 (a) x500 (b) x2000 .....	40
Figure 3. 11 SEM image of fractured surface of ABS-10-189 (a) x500 (b) x10000 .....	41
Figure 3. 12 Yield Strength and Elongation at Break values for ABS composite .....	44
Figure 3. 13 Yield Strength and Elongation at Break values for ABS-Blank and A-174 SCA treated serpentine filled ABS composite .....	44
Figure 3. 14 Yield Strength and Elongation at Break values for ABS-Blank and A-186 SCA treated serpentine filled ABS composite .....	45
Figure 3. 15 Yield Strength and Elongation at Break values for ABS-Blank and A-189 SCA treated serpentine filled ABS composite .....	45
Figure 3. 16 Comparison of Yield Strength values for all composites.....	46
Figure 3. 17 Comparison of Elongation at Break values for all composites.....	46
Figure 3. 18 Comparison of Young's Modulus values of ABS-Blank, ABS-2, ABS-5, ABS-10 and ABS-20.....	48
Figure 3. 19 Comparison of Young's Modulus values of ABS-2-174, ABS-5-174 and ABS-10-174.....	48
Figure 3. 20 Comparison of Young's Modulus values of ABS-2-186, ABS-5-186 and ABS-10-186.....	49
Figure 3. 21 Comparison of Young's Modulus values of ABS-2-189, ABS-5-189 and ABS-10-189 .....	49
Figure 3. 22 Impact Strength data of totally broken samples.....	51
Figure 3. 23 Melt flow index results for A-174 SCA treated serpentine filled ABS composite .....	53
Figure B. 1 DSC Thermograms of ABS-Blank, ABS-2, ABS-5, ABS-10 and ABS-20 .....	62
Figure B. 2 DSC Thermograms of ABS-2-174, ABS-5-174, ABS-10-174, ABS-2-186 ABS-5-186, ABS-10-186 .....	63
Figure B. 3 DSC Thermograms of ABS-2-189, ABS-5-189 and ABS-10-189 .....	64

# CHAPTER 1

## INTRODUCTION

### 1.1 Composite Materials

Composites are materials made from two different materials that remain as separate phases and where one of the materials is a binder or matrix and the other material is a reinforcement [1]. The advantage of composites is that they usually exhibit the best qualities of their components and often some qualities neither component possesses. Composite materials can be broadly classified into four different categories as laminated composite materials, particulate composite materials, fibrous composite materials and combinations of some or all of these three types [2].

Laminated composite materials (LCM) consist of two or more different materials that are bonded together. Lamination is used to combine the best aspects of the constituent layers. In “bimetal” type LCM, two different types of metals usually having significantly different thermal expansion coefficients are laminated to be used in temperature measurement devices. “Clad metals” is a kind of LCM in which one type of metal is sheathed in another. “Laminated glass” type is developed uniquely for automotive industry by placing polyvinyl butyral (a very tough and also flexible polymer) layer between two glass layers [2].

Particulate composite materials (PCM) consist of particles of one or more materials suspended in a matrix of another material. The type of composite is defined according to the type of matrix and particulate. They can be classified as both metallic or non-metallic. As a result of this classification, there are four types of

PCM: “Nonmetallic particles in nonmetallic matrix” (concrete – particles of sand and gravel that are bonded together with a mixture of cement and water), “Metallic particles in nonmetallic matrix” (solid rocket propellants – aluminum powder and perchlorate oxidizers in polyurethane or polysulfide rubber matrix), “Metallic particles in metallic matrix” (lead particles in copper alloys to improve machinability) and “Nonmetallic particles in metallic matrix” (cermet – ceramics suspended in a metallic matrix) [2].

As the name indicates, fibrous composite materials (FCM) uses fibers as the reinforcement part. Principal fibers used in FCM are glass, carbon (high modulus or high strength), aramid (or tradename as Kevlar – very light), boron (high modulus or high strength) and silicon carbide (high temperature resistant) fibers. Matrix materials chosen for FCM are polymers (thermoplastic and thermoset resins), minerals (silicon carbide, carbon) and metals (aluminium alloys, titanium alloys, oriented eutectics) [3].

## **1.2 Composite Materials Using Polymers as Matrix**

Although polymers have numerous advantages (such as light weight, ease of processing, cost etc.) over conventional materials, further improvements are being studied since 1950’s by combining polymeric materials with different materials. The studies resulted with two main categories of polymeric composites one of which can be named as “particulate filled polymer composites” and another one called “fiber reinforced polymer composites”.

Fibers used in advanced polymeric composites (continuous fibers; such as glass, carbon or graphite, aramid, high strength polyolefin, boron, silicon carbide fibers) have high aspect ratio, high stiffness and strength. These composites are used in primary structural applications and considered as high-performance structural materials. The fiber types (like whiskers), which are used in lightly loaded or secondary structural applications have lower values in properties mentioned above[4].

In these type of composites fibrous part has the roles of:

- carrying the load. In a structural composite, 70 to 90% of the load is carried by fibers.
- providing stiffness, strength, thermal stability, and other structural properties in the composites.
- providing electrical conductivity or insulation, depending on the type of fiber used.

On the other hand matrix material:

- binds the fibers together and transfers the load to the fibers providing rigidity and shape to the structure.
- isolates the fibers so that individual fibers can act separately stopping or slowing down the propagation of a crack.
- provides a good surface finish quality and aids in the production of net-shape or near-net-shape parts.
- provides protection to reinforcing fibers against chemical attack and mechanical damage (wear).[5]

### **1.2.1 Particulate Composites with Polymer Matrix**

Traditionally, “fillers” are considered as additives which moderately increase the modulus of the polymer without an improvement in strength (tensile, flexural) because of their geometrical features, surface area or chemical composition. They mainly reduce cost by replacing with the more expensive polymer and faster molding cycles by increasing thermal conductivity [6].

However “reinforcing fillers” are discontinuous additives of which form, shape, and/or surface chemistry have been suitably modified with the objective of improving the mechanical properties of the polymer, particularly strength [6].

Particulate filler materials can be categorized under two subgroups; “Mineral Fillers”, “Synthetic Particulate Fillers”.

### **1.2.1.1 Mineral Fillers**

Mineral fillers are a vital and significant part of the world’s polymer industry. Consumption in rubber and plastics is currently estimated to be over 2.5 million tonnes per year in Western Europe [7]. The types of mineral fillers in general are: Calcium Carbonate Minerals, Dolomite, Kaolin, Calcinated Clay, Mica, Talc, Montmorillonite, Barite, Calcium Sulfate Products, Wollastonite and Crystalline Silicas. The most important mineral fillers used are carbonates, clays and talcs [7].

Calcite (calcium carbonate) and dolomite (calcium-magnesium carbonates) are the main carbonate fillers used in industry [7]. They primarily reduce costs together with affecting mechanical properties in a little portion. However on particular polymer systems, they may be considered as multifunctional fillers with various effects on rheology, processing and morphology [6]. Main matrix materials applied are PVC (nearly 80%), thermosets and fiber glass reinforces unsaturated polyesters.

Clay minerals are aluminium silicates of either the two-layered kaolinite type or three-layered montmorillonite type. Two clay minerals are commonly used in the polymer industry, which are namely montmorillonite and kaolinite.

Montmorillonite, also known as bentonite which is a member of phyllosilicate minerals (layer silicate) is the main raw material for nanocomposite studies with polymeric materials. It is shown that nano sized montmorillonite addition to polymers results in an improvement in mechanical properties, thermal and barrier properties and fire resistance [7].

Kaolin which is also a member of phyllosilicates is widely known as “China clay” [8]. Kaolin, which is a plate-like filler has a relatively low aspect ratio. It imparts certain mechanical property improvements to thermoplastics. Like other plate-like

materials, kaolin can improve dimensional stability (warp resistance), isotropy, and surface smoothness, a common problem with high aspect ratio fibrous reinforcements [6].

Talc, natural mineral found worldwide is the major constituents of rocks known as soapstone and staeatite [9]. Talc has the lowest hardness value of minerals as 1 in the Mohs Hardness Scale. Primary reasons for using talc include improvements in mechanical properties such as heat deflection temperature (HDT), rigidity, creep resistance, and sometimes impact resistance, as well as lower shrinkage. Additional secondary benefits include improvements in dimensional stability and lower permeability [6].

### **1.2.1.2 Synthetic Particulate Fillers**

Synthetic particulate fillers are composed of carbon black, synthetic silicas (precipitated and fumed silica), aluminium hydroxide, magnesium hydroxide and antimony oxides. The main interest is focused on carbon black filler upon all synthetic particulate fillers. Precipitated silica and fumed silica are used as reinforcing filler in hydrocarbon and silicone elastomers, aluminium and magnesium hydroxide are used as flame-retardant fillers in elastomers, thermosets and some thermoplastics and antimony oxides (antimony trioxide and pentoxide) are also used as flame-retardant fillers [6].

Carbon blacks are soots produced by incomplete combustion of volatile organic materials, principally oil and gas [6]. They are mainly used for reinforcing agents for elastomers, especially in automotive tires (90% of the utilization). Other areas of application are conductive fillers, pigments and stabilizers for outdoor usage.

## **1.3 Layered Silicate Minerals**

Layered silicate minerals (phyllosilicates or sheet silicates) include a group of minerals which has  $Mg^{2+}$ ,  $Fe^{2+}$ ,  $Fe^{3+}$ ,  $Ni^{2+}$  and  $K^+$  in their composition besides silica.

Their structure can be regarded as a result of the combination of tetrahedral and octahedral layers. They contain hydroacids of the  $(OH)^-$  group and other additional anions and water. Tetrahedral represents a hexagonal net of silicon-oxygen tetrahedrons in which three of the four oxygen ions are common. The second layer, octahedral is formed by the ions of aluminium, magnesium or iron that are in the octahedral coordination (Figure 1.1) [10].

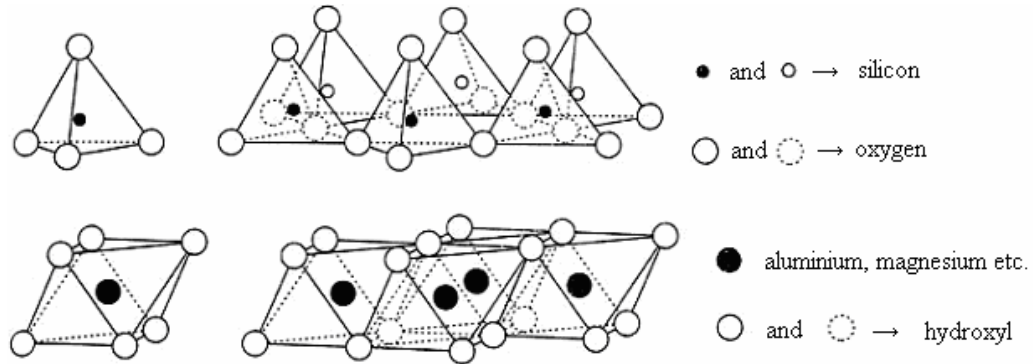


**Figure 1.1** A single tetrahedral (up side left), a sheet structure of silica tetrahedral arranged in a hexagonal network (up side right), a single octahedral unit (down side left) and a sheet structure of octahedral units (down side right)

Two, three and multilayer structural types of layered silicates are present. They can be distinguished according to the kind of relationship that exists between the tetrahedral and octahedral layers. The packets in the 1:1 type layered silicates are composed of one tetrahedral and one octahedral layer. Serpentine and kaolin minerals are of this type of mineral. In three-layered silicates (2:1) the packets consist of two tetrahedral layers and one octahedral layer situated between them. In the multilayer types (2:1:1) structure is constituted by a layer of brucite  $Mg(OH)_2$  or gibbsite  $Al(OH)_3$  in the interlamellar space (Figure 1.2) [10].

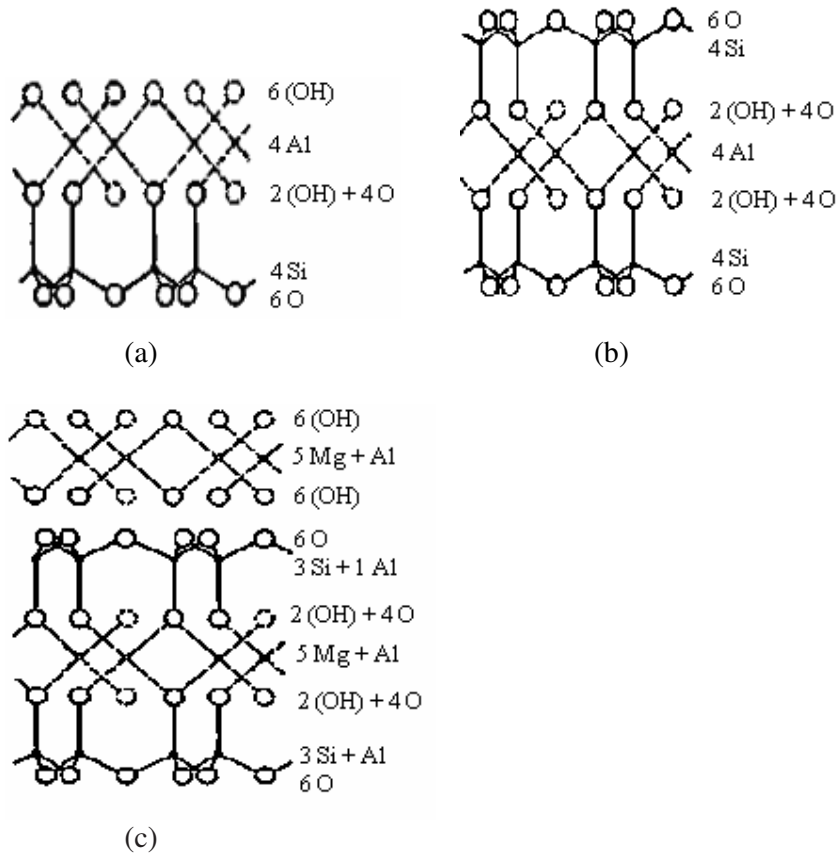
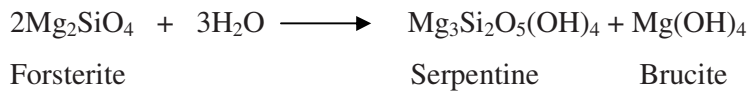


**Figure 1.** 2(a) 1:1 – Kaolinite -  $\text{Al}_4\text{Si}_4\text{O}_{20}(\text{OH})_8$  (b) 2:1 – Montmorillonite -  $\text{Al}_4(\text{Si}_4\text{O}_{10})_2(\text{OH})_8 \cdot x\text{H}_2\text{O}$  (c) 2:1:1 – Chlorite –  $\text{Mg}_{10}\text{Al}_2(\text{Si}_6\text{Al}_2)\text{O}_{20}(\text{OH})_{16}$

### 1.3.1 Serpentine

Serpentine mineral is a member of 1:1 layer type phyllosilicates. Its general formula is  $\text{Mg}_3\text{Si}_2\text{O}_5(\text{OH})_4$  but it usually contains the impurities of  $\text{Fe}^{2+}$ . In the crystalline structure of serpentine, the layers of hexagonal networks are composed of silicon-oxygen tetrahedrons from two layered packets combining with the octahedral layer in which  $\text{Mg}^{2+}$  ions are in an octahedral environment of  $2\text{O}^{2-}$  and  $4(\text{OH})^-$  ions. Three polymorphs of serpentine are found; antigorite, lizardite and chrysotile. It is recognized by its variegated green color and its greasy luster or by its fibrous nature. Serpentine is a widely distributed mineral found in nature (Canada, South Africa, Russia, Greece, England, Turkey, etc.) usually as an alternation of magnesium

silicates, especially olivine, pyroxene and amphibole. It may form by the reaction from forsterite as follows:



Antigorite and lizardite are generally massive and fine-grained however chrysotile is fibrous. The asbestiform variety, chrysotile constitutes the world's approximately 90-95% of the asbestos deposit. Before it is found to be carcinogen by International Agency for Research on Cancer, it was mined in lots of different locations to be used as fireproofing and as an insulation material against heat and electricity. Massive serpentine is often used as an ornamental stone and may be valuable as building material [10-12].

#### 1.4 Silane Coupling Agents

The natural surfaces of some type of the reinforcing elements are less than optimum for dispersion into polymers and for interaction with polymers. Furthermore, it must be kept in mind that the surface of the reinforcing element plays a crucial role in determining the properties and processing behaviour of composites.

Silane coupling agents are the most widely used surface modifiers especially in plastics industry. Following performance benefits can be obtained by silane coupling agents: modified surface characteristics (hydrophobicity), improved dimensional stability, improved filler dispersion (no agglomeration), increased wet-out between resin and filler, improved mechanical properties and controlled rheological properties [6].

Common silanes have the general formula  $\text{Y}-(\text{CH}_2)_3\text{Si}(\text{X})_3$  represented in Figure 1.3 and  $\text{Y}-(\text{CH}_2)_2\text{Si}(\text{CH}_3)(\text{X})_2$ . The silicon functional group X is a hydrolyzable group chosen to react with surface hydroxyl groups of the filler to produce a stable bond, and is usually halogen or alkoxy. The organofunctional group Y is tightly bound to

the silicon with a short carbon chain and links with the polymer. This group has to maintain maximum compatibility with the resin system. Bonding to the polymer takes place by chemical reactions or physicochemical interactions such as hydrogen bonding, acidbase interaction, interpenetration of the polymer network (entanglement), or electrostatic attraction. The group Y may be non-functional or functional (reactive) [6].

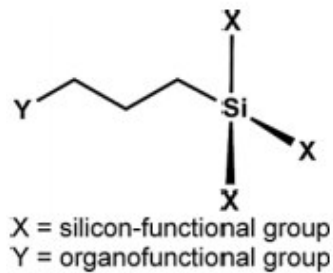


**Figure 1.3** General structure of organosilanes

### 1.4.1 Silane Coupling Agents & Fillers

Organosilanes utilize the reaction with surface hydroxyl groups to produce a stable covalent bond and a stable layer on the filler surface (Figure 1.4). Thus, they are most effective on fillers with high concentrations of reactive hydroxyls and a sufficient amount of residual surface water. Silica, silicates (including glass), oxides, and hydroxides are most reactive towards silanes.

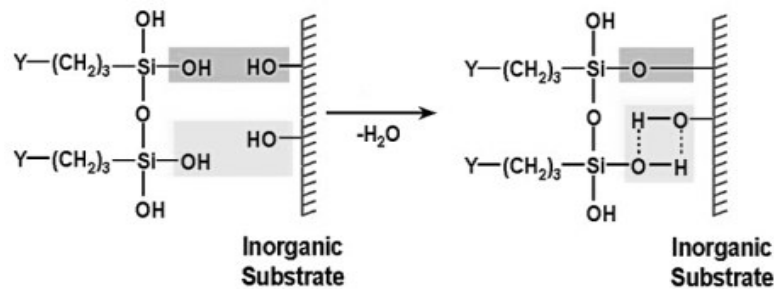


**Figure 1.4** Mode of reaction between a silanol and an inorganic surface

Firstly, fixation of the silanol on the filler surface is accomplished through hydrogen bonding with the surface OH groups. Until the water molecule is eliminated, this reaction is thought to be reversible. As long as there is only hydrogen bonding, the silane can still remove on the filler surface. The covalent bond [silane–O–filler] fixes the silane on the filler surface. The silane form a monolayer on the filler surface. Explaining the exact nature of the surface layers and their relationship with the coating conditions is very hard. The current understanding is that silane layers on mineral surfaces are thicker than the theoretical monolayer (Figure 1.5). Such layers are very complex and depend on the coating conditions used, the nature of the mineral surface, and the chemistry of the reactive functionalities present [6].

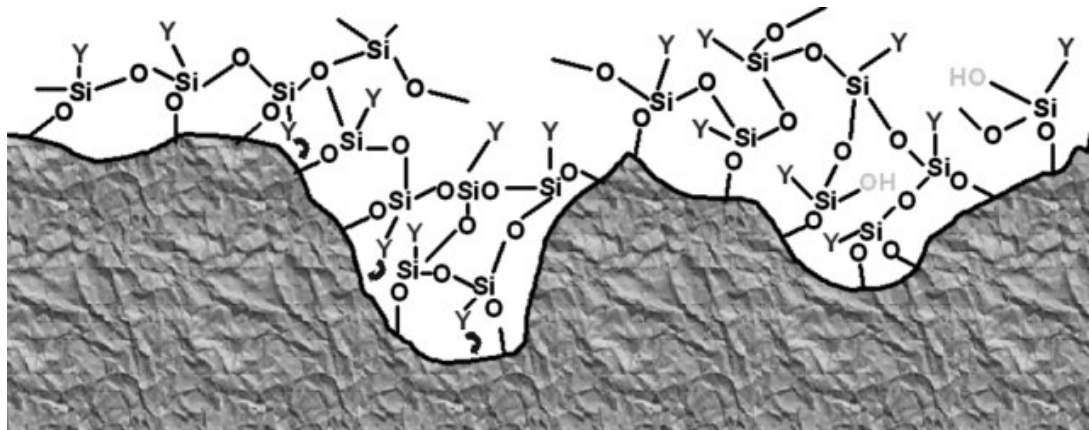


**Figure 1. 5** Overview of a silanized surface

## 1.4.2 Types of Silane Coupling Agents

### 1.4.2.1 Vinylsilanes

These types of silanes have the hydrolyzable group of methoxy, ethoxy, 2-methoxyethoxy or acetoxy generally. They are applied to polymers that are cross-linked by a free radical process (peroxide cure) [7].

#### **1.4.2.2 Methacryloxysilanes**

Methacryloxysilanes provide more reactive forms of unsaturation than vinylsilanes. They are used extensively in free-radical curing formulations where extra reactivity is needed. Commercial products usually contain  $\gamma$ -methacryloxypropyl groups. Their major advantage is to decrease the viscosity of the applied composite [7].

#### **1.4.2.3 Epoxysilanes**

3-glycidoxypropyltrimethoxysilane is the main epoxy type silane coupling agent. They are relatively expensive and are principally used in epoxies for which they are superior to other silane coupling agent types. Like methacryloxysilanes, reduction in viscosity value is the best feature of epoxysilanes other than surface improvement [7].

#### **1.4.2.4 Aminosilanes**

Aminosilanes are widely used types of silane coupling agents with an application area including epoxies, phenolics, urethanes, polyamides, some thermoplastic polyesters and elastomers. The commercial ones are usually based on  $\gamma$ -aminopropyl functionality. They give great stability to aqueous solutions unlike most silanes [6,7].

#### **1.4.2.5 Sulfur Functional Silanes**

This silane coupling agents are specifically designed for sulfur curing elastomer systems. However they are still used in considerable amounts in industry. Two principal forms are  $\gamma$ -mercaptopropylsilane and various polysulfidic silanes (especially tetrasulfide). Although both two types are very effective, mercaptosilane

is the most efficient one. There has been a remarkable growth in the use of the tetrasulfide due to its key role with precipitated silica in the development of low rolling resistance or green tyres [7].

### **1.5 Acrylonitrile – Butadiene – Styrene (ABS)**

ABS copolymer is the copolymerization product of three polymers; acrylonitrile, butadiene and styrene. ABS is patented in 1948 by United States Rubber Company as a “Composition of butadiene-acrylonitrile copolymer and styrene-acrylonitrile copolymer”. From the beginning of 1950s till today it is an important thermoplastic utilized in many areas like house-hold appliances, camera housings, telephone handsets, automotive industry, pipe and fittings, refrigerator liners. It is the fourth thermoplastic (after polyethylene, polypropylene, polyvinyl chloride and polystyrene) in terms of annual production rate and sales in the U.S [13].

Monomers ratios and production techniques may vary but there are two basic properties which characterize ABS plastics materials; good-to-excellent toughness and high mechanical strength. All variations of ABS polymers have these two properties in common. If the contributions are investigated monomer by monomer; acrylonitrile gives chemical resistance, heat resistance and high strength; butadiene contributes toughness, impact strength and low-temperature property retention; styrene gives rigidity, surface appearance (gloss) and processability [14].

Two paths are followed in ABS manufacture which are blends of styrene-acrylonitrile copolymers with butadiene-acrylonitrile rubber and interpolymers of polybutadiene with styrene and acrylonitrile (Figure 1.7). The latter is dominantly applied way of producing ABS.

First method is applied via simple melt mixing of two types of copolymers mentioned above. A typical blend consists of 70 parts styrene-acrylonitrile (70:30) copolymer and 40 parts butadiene-acrylonitrile (65:35) rubber.

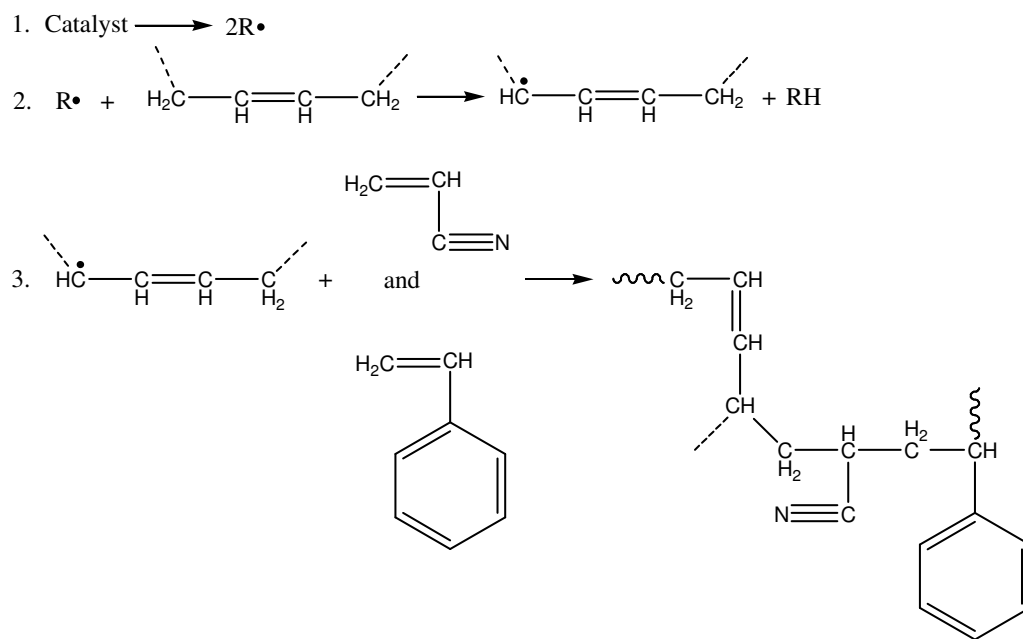


**Figure 1. 6** Grafting reaction of butadiene onto SAN [14]

Interpolymers are produced by copolymerizing styrene and acrylonitrile in the presence of butadiene rubber by using batch or continuous emulsion polymerization (Figure 1.6). The resultant materials are a mixture of polybutadiene, SAN copolymer and polybutadiene grafted with styrene and acrylonitrile. The mixture is made up of three phases: a continuous matrix of SAN, a dispersed phase of polybutadiene and a boundary layer of SAN graft. The graft polymer provides the link between the other two components and therefore responsible for improving the properties of the mixture. Because of the similarity in chemical compositions between SAN copolymer and SAN monomers grafted onto the polybutadiene molecule, these two components are soluble. This provides the mechanical bonding between the rigid and the rubbery phase. The resulting polymer in this production technique may vary in SAN-rubber ratio, the styrene to acrylonitrile ratio in the SAN component, the amount of grafted SAN, rubber particle size and particle size distribution, cross-link density of the rubber, use of modified styrenes such as  $\alpha$ -ethyl styrene to increase heat deflection temperatures, use of saturated rubbers instead of polybutadiene to improve weatherability [11,15,16].

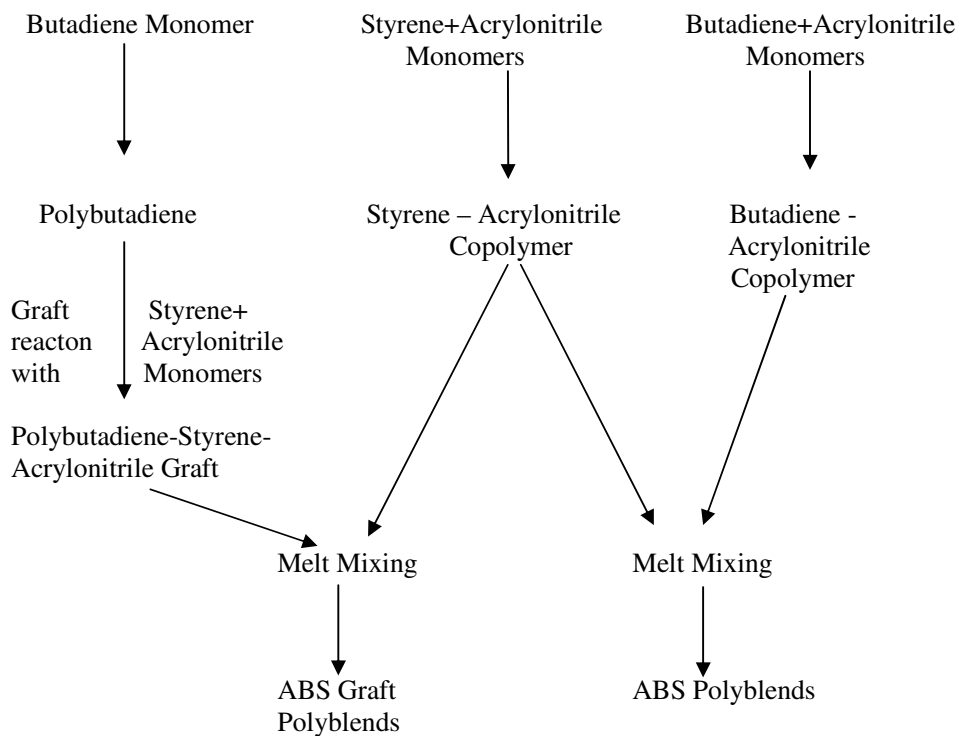


**Figure 1. 7** Chemical steps involved in the preparation of ABS

### 1.5.1 Special Grades of ABS

For the purpose of being a suitable plastic for various applications, special grades of ABS resin are developed and adopted for these different requirements. These alterations can be generally done by variation in the monomer compositions or blending with another polymer to improve the relatively weak properties.

Being a multiphase polymer blend, the effects of the compositional and structural features in ABS are complex and interdependent. However some investigated variations have clear results. Shifting the AN content of SAN from 20-30%, which most general purpose ABS contain, to 35% improves chemical resistance significantly. It is also indicated that AN in SAN improves the crazing resistance of SAN, creep and fatigue performance also improve as the AN content of the SAN is

increased. On the other hand, increasing the molecular weight of the SAN matrix increases impact toughness. It is also found that the rubber particle volume fraction alone is the most important parameter controlling modulus values of ABS resins since the modulus of rubber is almost 1000 times smaller than the modulus of the matrix SAN [17].

ABS is blended with polycarbonate to obtain high dimensional stability, low shrinkage, low moisture absorption, high stiffness and hardness, good electrical properties in the low voltage and low power range and good impact resistance at temperatures starting from -50°C. Another common example for blending is the addition of polyvinyl chloride to ABS. These blends offer excellent processability, high impact strength, UV stability, flame resistance, weatherability at a low cost, and excellent cost-to-performance ratio. Blending of ABS with an acrylic material such as poly(methyl methacrylate) can allow a matching of the refractive indices of the rubbery and glassy phases and provides a low level of contaminating material such as soap and in absence of insoluble additives, a reasonable transparent ABS-type polymer may be obtained. Furthermore, ABS is blended with thermoplastic polyesters for obtaining excellent moldability, stress-crack resistance, high gloss, low shrinkage, good dimensional stability, good wear and abrasion resistance, good thermal, weathering and solvent resistance (to gasoline and motor oils). Another blend is ABS with polyamides in the presence of compatibilizer because of high immiscibility. These blends shows good processability and flow, good surface finish (gloss or matte as required), high heat, chemical, oil, wear and abrasion resistance, dimensional stability, low temperature impact strength, reduced moisture sensitivity and economy [13,18,19].

#### **1.5.2.1 ABS – Filler Composite Studies**

Jiang et al.[20] studied with ABS, reinforced by micron-size (MCC) and nano-size precipitated calcium carbonate particles (NPCC) through melt compounding for investigating mechanical properties. They found that MCC have higher modulus but

lower tensile and impact strength than neat ABS. However, NPCC increased modulus of ABS while maintained its impact strength due to larger interfacial area and cavitation toughening.

ABS-metallic powder or filament and ABS-carbon fiber composites are used in electromagnetic interference (EMI) shielding studies. Lu G. et al.[21] studied the electrical conductivity and shielding effectiveness of nickel coated carbon fibers-ABS composites. As the fiber content increased in the composite of Ni-coated carbon fibers-ABS, the resistivity decreased. At the same fiber content, the conductivity of the composites filled with Ni-coated carbon fibers was much greater than that of ordinary carbon-filled composites. It was understood that to reach the same resistivity with carbon-fiber-filled composites, the use of Ni-coated carbon fibers as filler can greatly decrease the required volume fraction of fibers. The shielding effectiveness of ABS resin filled with 10 vol% of Ni-coated carbon fibers was about 50dB. On the other side Tzeng et al.[22] studied EMI effectiveness of copper and nickel-coated carbon fiber-reinforced ABS composites. They observed that lengths of nickel coated carbon fibers are smaller than the copper coated carbon fibers. As a result their composites showed superior EMI shielding effectiveness with respect to copper coated ones due to excellent bonding between nickel coating and fibers together with longer fiber length distribution.

Liang [23] studied tensile and flexural properties of silane coupling treated hollow glass bead-filled ABS composites. He observed an approximately linear increase in Young's modulus, an increase in tensile and flexural strength up to 5% volume fraction of addition and a decrease in that values after volume fraction of addition was over 5%.

Tjong et al.[24] studied mechanical and thermal properties of tetrabutyl orthotitanate treated potassium titanate whisker filled ABS composites. They found that both modulus and stress at break increased, impact strength was decreased with increasing whisker content and strain at break was not affected significantly. Furthermore, it was understood that potassium titanate whiskers have a little effect on the thermooxidative stability of ABS.

Gülsoy et al. [25] investigated physical and mechanical properties of bronze powder filled ABS composite. They found that yield and tensile strength, percent elongation, impact strength, melt flow index values were decreased and elasticity, hardness, vicat softening point and heat deflection values were increased with increasing bronze volume percentage in the composite.

Kim et al. [26] studied the synergistic effect of triphenyl phosphate nanocomposite (TPP),(synthesized by intercalating TPP into galleries of mica-type silicates) epoxy resin and silane coupling agent mixtures on thermal stabilization enhancement of ABS. TPP addition alone slightly improved the thermal stability, however epoxy resin together with TPP resulted with a significant decrease in limiting oxygen index. Further enhancement is obtained by the addition of silane coupling agent as the third component. In this study, another phosphorus type flame retardant, tetra-2,6-dimethylphenyl resorcinol diphosphate (DMP-RDP), is also used and an LOI as high as 44,8 was obtained after synergistic effect of epoxy resin and silane coupling agent addition.

Liu B. et al. [27] investigated the thermal stability, flame retardancy and rheological behavior of magnesium hydroxide sulfate hydrate (MHSH) whisker-ABS composite and the effect of zinc stearate as a dispersion additive for ABS/MHSH composite. Addition of zinc stearate improved the dispersion of MHSH in ABS matrix. Heat release rate and mass loss rate are considerably decreased with increasing whisker content while composites with zinc stearate has much more lower heat release rate. Viscosity and the storage modulus were increased at low frequency zone with increasing MHSH content and ABS/MHSH composites exhibit distinct solid-like response at terminal zone than ABS.

#### **1.5.2.2 ABS – Clay Composite Studies**

Wang et al. [28,29,30] studied firstly on preparation and thermal properties of ABS/montmorillonite nanocomposite. Direct melt intercalation was applied and they

obtained a kind of intercalated-delaminated nanocomposite structure and TGA results proved that an improvement in char formation and thermal stability was achieved. In a different work, they chose particle size of montmorillonite as the variable. 5 $\mu\text{m}$  and 38 $\mu\text{m}$  particle sizes were selected, ABS/5% nanocomposites were prepared and their structure and flammability properties were investigated. It is observed that 5 $\mu\text{m}$  sized nanocomposite had a kind of intercalated-delaminated structure, whereas 38 $\mu\text{m}$  sized nanocomposite had an intercalated structure. Both nanocomposite showed a lower heat release rate peak and higher thermal stability than neat ABS. In addition exfoliated-intercalated nanocomposite performed a better fire retardancy characteristic. Another study was made to compare the thermal stabilities of ABS/MMT nanocomposites with ABS/MMT nanocomposites with conventional fire retardants decabromodiphenyl oxide and antimony oxide. The latter showed a lower heat release rate peak and higher limiting oxygen index value.

Ma et al. [31] studied morphologies, thermal stability and flammability properties of ABS-graft-maleic anhydride/clay nanocomposites. The size of dispersed rubber domains of ABS-g-maleic anhydride and the uniformity of dispersion was increased with respect to neat ABS. An intercalated/exfoliated structure was obtained. This intercalated/exfoliated structure of ABS-g-maleic anhydride/OMT had better barrier properties and thermal stability than intercalated ABS/OMT nanocomposites. Furthermore, ABS-g-maleic anhydride/OMT nanocomposite had a significantly low flammability compared with ABS/OMT nanocomposite.

Patino-Soto et al. [32] studied morphological and thermal properties of ABS/clay nanocomposites with two different acrylonitrile content and three different organo-modified clays (Cloisite 10A, 20A and 30B-with three different quaternary ammonium salts) plus natural sodium clay. Results showed that the ABS with higher acrylonitrile content produced a greater intergallery spacing due to greater polarity. On the other hand, the greater clay intergallery spacing was obtained from Cloisite 20A (very slightly polar) which had greater intergallery spacing initially. However the greater increase in intergallery spacing (from initial spacing in the plain clay to the final nanocomposite) was obtained from Cloisite 30B which contains most polar

organo-modifying groups. Cloisite 20A and 30B modified ABS/clay nanocomposites with higher acrylonitrile content produced nanocomposites with higher storage modulus, higher degradation temperature and better flame retardancy. It was understood that polarity and intergallery spacing plays an important role in determining dispersion.

Choi et al. [33] studied the role of laponite, the second clay with montmorillonite, as a colloidal stabilizer in ABS/clay nanocomposites. Laponite, being a low aspect ratio clay, reduced the particle sizes of ABS/clay nanocomposite latexes, enhanced colloidal stabilities and increased viscosity of the latexes. ABS/clay nanocomposites showed exfoliated structures and as ratio of sodium montmorillonite to laponite was increased in nanocomposite, dynamic moduli was increased because sodium montmorillonite had higher aspect ratio than laponite.

## **1.6 Aim of the Study**

The aim of this study is to prepare and characterize serpentine filled ABS composites. SCA treated and non-treated serpentine filled composites, having different filler compositions were prepared and their morphological characterization by scanning electron microscopy, mechanical characterization by tensile and impact testing, thermal characterization by differential scanning calorimetry and flow characterization by melt flow index tests were done.

## CHAPTER 2

### EXPERIMENTAL

#### 2.1 Materials

##### 2.1.1 Acrylonitrile Butadiene Styrene Copolymer

ABS was used as polymer matrix in this study and it was obtained from Arçelik as LG HF 380 grade. As the abbreviation indicates (HF-high flow), good flowability and excellent processibility are key characteristics of this grade. It is utilized in the applications such as; air-conditioner, telephone, electric fan, mixer, toy, kitchen good. Table 2.1 shows some of some properties of LG HF 380 grade ABS polymer.

**Table 2. 1** Some properties of ABS

Property	Method	Condition	Unit	Value
Melt Flow Index	ASTM D1238	220°C / 10 kg	g/10 min	43
Specific Gravity	ASTM D792	23°C	-	1,04
Mold Shrinkage	ASTM D955	-	%	0.4 ~ 0.7
Tensile Strength at Yield	ASTM D638	50mm/min	kg/cm <sup>2</sup>	450
Elongation at Yield	ASTM D638	50mm/min	%	>5
Elongation at Break	ASTM D638	50mm/min	%	>10
IZOD Impact Strength	ASTM D256	1/4", 23°C	kg.cm/cm	25
Rockwell Hardness	ASTM D785	R-Scale	-	106
Heat Deflection Temp.	ASTM D648	1/4", 18.5 kg	°C	86

**Table 2.1** (Continued)

<b>Property</b>	<b>Method</b>	<b>Condition</b>	<b>Unit</b>	<b>Value</b>
Vicat Softening Temperature	ASTM D1525	5kg, 50°C/hr	°C	94
Flammability	UL94	1/8"	class	HB

### **2.1.2 Serpentine**

Serpentine mineral was used as the filler in this study. It was collected from Beynam region in Ankara. The mineral was collected in its natural size and size reduction procedure was carried out. The detailed information was given in Ph. D. Thesis of S. Tan [34].

### **2.1.3 Silane Coupling Agents**

Three different types of SCA, A-174, A-186 and A-189, were applied to serpentine in order to increase the interaction between the interphases of clay and polymer. They are obtained previously from Union Carbide Company, which does not exist on the market presently. Chemical structures and some properties of the SCA are listed below in Figure 2.1 and in Table 2.2, respectively.

A-174,  $\gamma$ -methacryloxypropyltrimethoxysilane, has methacryloxy functionality. This SCA was selected for application due to suitability of usage with ABS stated in information sheet of the company.

A-186,  $\beta$ -(3,4-epoxycyclohexyl)-ethyltrimethoxysilane has epoxy functionality. This SCA was also selected due to the same reason stated for A-174.

A-189,  $\gamma$ -mercaptopropyltrimethoxysilane, has mercapto or sulfur containing functionality. This SCA was chosen in order to make comparison between other applied silane coupling agents.

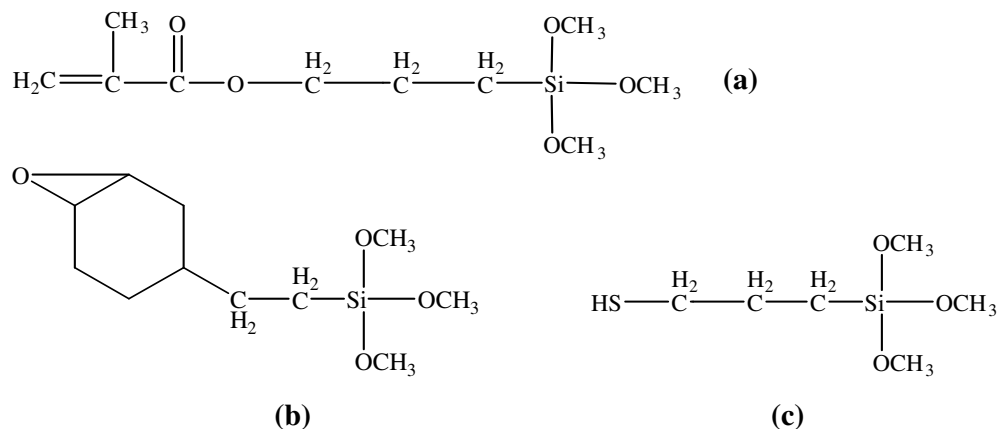


**Figure 2. 1** Chemical Structures of (a) A-174 (b) A-186 and (c) A-189

**Table 2. 2** Properties of SCAs

Property	A-174	A-186	A-189
Specific Gravity	1,045	1,065	1,057
Viscosity @ 25°C (cp)	2	5,2	2
Boiling Point at 760 mm Hg (°C)	255	310	--
Solubility in Acetone	Soluble	Soluble	Soluble
Solubility in Benzene	Soluble	Soluble	Soluble
Solubility in Ethyl Ether	Soluble	Soluble	Soluble
Solubility in Water	Reacts	Reacts	Reacts

## 2.2 Experimental Procedure

During this study, the first step was the particle size reduction of serpentine mineral. Then SCA treatment was applied with three types of silanes. Composites with different compositions were prepared by extrusion. Prepared composites were injection molded for characterization purposes.

### 2.2.1 Size Reduction of Serpentine

Tan [34] studied nanocomposite production of serpentine and polypropylene. In that study, serpentine, collected from Beynam region in Ankara, was hammered, ground, rolled and pulverized respectively in order to reduce the particle size. Before further size reduction of as received pulverized serpentine (which was obtained from Tan's study) was done in this study, it was wet sieved with ethanol by using 400 mesh (38  $\mu$ ) screen. Serpentine collected from sieving was dried and finally ball milling in aqueous ethanol medium was done. After all size reduction procedures, particle sizes were measured with Malvern Mastersizer 2000 and the following results were found.

**Table 2. 3** Final value of average particle size of serpentine powder after size reduction process

<b>d (0.1)</b>	<b>d (0.5)</b>	<b>d (0.9)</b>
1.204 $\mu\text{m}$	3.302 $\mu\text{m}$	8.772 $\mu\text{m}$

### 2.2.2 Silane Coupling Agent Treatment

2 weight-% (SCA/[serpentine+SCA]) A-174, A-186 and A-189 treated serpentine minerals were prepared. Firstly, required amount of SCA was dissolved in 50cc ethylacetate to obtain 2.5 weight-% (SCA/[SCA+ethyl acetate]) mixture.

Ethylacetate was >99.5% pure because SCA have a risk to react with water. The stock solution of SCA/Ethyl acetate was added into the micron sized serpentine and they were mechanically mixed. Then controlled evaporation of the mixture was carried out till the ethyl acetate was removed from the mixture.

### 2.2.3 Melt Mixing by Extrusion

ABS/treated and untreated serpentine were mixed by using a twin screw extruder with a model of Thermoprism TSE 16 TC. It is a co-rotating, twin screw extruder having an L/D ratio of 24. Moisture content of ABS is removed prior to extrusion by drying ABS pellets at 85°C for 4 hours. Serpentine and ABS was fed to the extruder from separate feeders. Table 2.4 shows the extrusion process variables and Table 2.5 lists the prepared composites.

**Table 2. 4** Extrusion process variables

<b>Process Variable</b>	<b>Value</b>
Barrel Temperatures (from hopper to die, respectively) , °C	160 – 170 – 190 - 200 - 220
Screw Speed, rpm	250
Feed Rate (ABS+Serpentine) , g/min	20

**Table 2. 5** Prepared ABS-Serpentine Composites, compositions and SCA contributions

<b>Sample Code</b>	<b>ABS Content (%)</b>	<b>Serpentine Content (%)</b>	<b>A-174</b>	<b>A-186</b>	<b>A-189</b>
<b>ABS-Blank</b>	100	--	--	--	--
<b>ABS-2</b>	98	2	--	--	--
<b>ABS-5</b>	95	5	--	--	--
<b>ABS-10</b>	90	10	--	--	--
<b>ABS-20</b>	80	20	--	--	--
<b>ABS-2-174</b>	98	2	✓	--	--
<b>ABS-5-174</b>	95	5	✓	--	--
<b>ABS-10-174</b>	90	10	✓	--	--
<b>ABS-2-186</b>	98	2	--	✓	--
<b>ABS-5-186</b>	95	5	--	✓	--
<b>ABS-10-186</b>	90	10	--	✓	--
<b>ABS-2-189</b>	98	2	--	--	✓
<b>ABS-5-189</b>	95	5	--	--	✓
<b>ABS-10-189</b>	90	10	--	--	✓

#### **2.2.4 Injection Molding**

Injection molding was carried out by using a laboratory scale injection molding machine, Daca Instruments Micro Injector. Pelletized composites were dried for 4 hours before they were injection molded. The barrel temperature and mold temperature was set to 220°C was set to 80°C, respectively.

## 2.3 Sample Characterization

Prepared samples were analyzed in terms of structural, mechanical, thermal and flow characteristics for investigating the changes after addition of filler to the polymer. Scanning electron microscopy (SEM) was done for structural characterization, tensile testing, impact testing are done for mechanical characterization, differential scanning calorimetry (DSC) is done for thermal characterization and melt flow index (MFI) test is done for flow characterization.

### 2.3.1 Tensile Testing

Instron Tensile Testing Machine TM1102 was used for tensile testing. Injection molded dumbbell specimens (Figure 2.2) having dimensions in the Table 2.6 were used in the testing. The drawing rate was 50 mm/min and tests were done at room temperature.

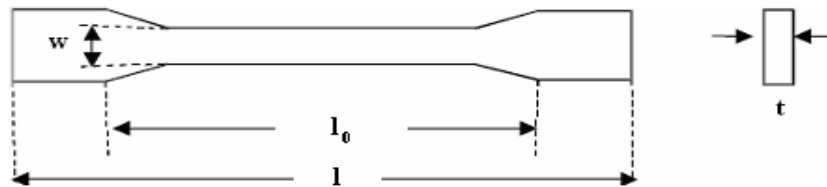


**Figure 2. 2** Representation of a dumbbell shaped specimen

**Table 2. 6** Dimensions of dumbbell specimen

Abbreviation	Value
$l_0$ , Distance between grips, mm	80
$l$ , total length of sample, mm	112
$w$ , Width of sample, mm	7
$t$ , thickness of sample, mm	2

### **2.3.2 Impact Testing**

Injection molded specimen having dimensions of 60mm x 7mm x 2mm were used in unnotched charpy impact test. Tests were performed by using a pendulum impact tester of Coesfeld Testing Machine according to ASTM D256 at room temperature.

### **2.3.3 DSC**

Thermal properties of specimen were investigated with DSC test under nitrogen atmosphere. The test machine was Dupont Thermal Analyst 2000 DSC 910S. Measurements were done in the temperature interval of 25 to 250°C at a scanning rate of 20°C/min.

### **2.3.4 MFI**

Melt flow index test was done under 2.16 kg load at 220°C by using a Coesfeld Material Test, Meltflicker LT according to ASTM D1238.

### **2.3.5 SEM**

SEM analysis was done by using a JEOL JSM-6400 model low voltage scanning electron microscope. The fracture surface of the tensile testing specimen from all types of concentrations were analyzed in this test. In order to achieve electron transfer, a thin layer of gold was applied to all specimen.

## CHAPTER 3

### RESULTS AND DISCUSSION

#### 3.1 Morphological Characterization

Morphological characterization of composites was done by SEM analysis. Surfaces of the samples fractured in tensile testing were used in SEM analysis.

##### 3.1.1 Scanning Electron Microscopy Analysis

SEM analysis was used to examine surface characteristics, homogeneity of dispersion of serpentine particles in ABS matrix, modification of the interaction on the polymer-clay interface after SCA treatment and to visually observe particle size distribution which was obtained experimentally. Micrographs of composites are given for ABS-5, ABS-10, ABS-20, ABS-2-174, ABS-5-174, ABS-10-174, ABS-2-186, ABS-5-186, ABS-10-186, ABS-5-189 and ABS-10-189 from Figure 3.1 to Figure 3.11, respectively.

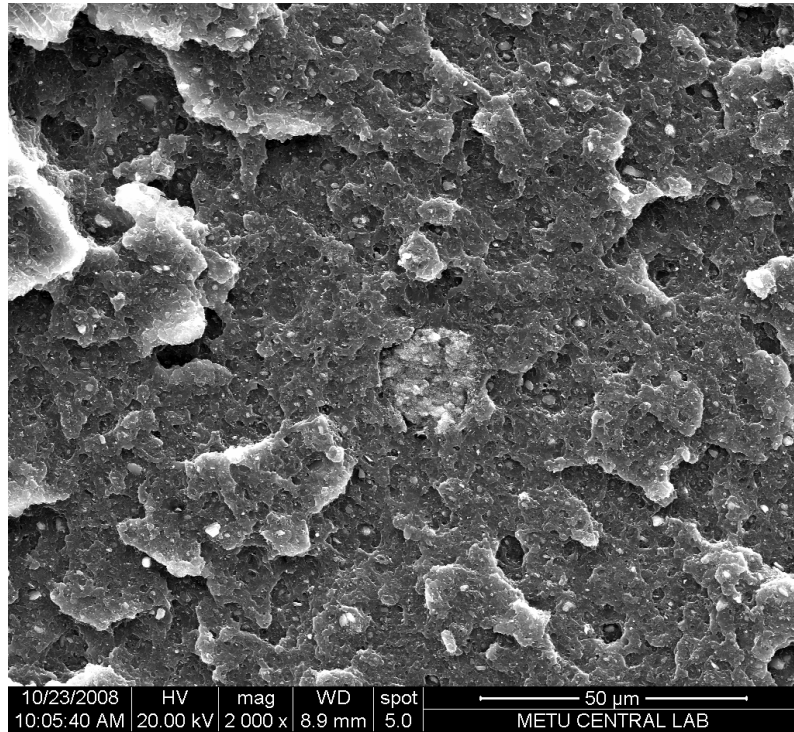
Micrographs of non-treated serpentine filled composites are given in Figure 3.1 to Figure 3.3. There is a homogeneous distribution of filler through matrix. Weak interaction on the interface of serpentine and ABS, and large cavities and holes with varying sizes were observed in Figure 3.2.b. Figure 3.3.a gives an idea about the homogeneity of the distribution of clay particles. Nevertheless, a serpentine particle having an approximate diameter of 20 $\mu$ m embedded in ABS matrix can be seen in Figure 3.2.b. This particle, because of its unusual big size, remained in the fracture surface although it shows no clue of adhesion with polymer matrix.

Starting from Figure 3.4 to Figure 3.6, A-174 SCA treated serpentine filled composites are given. All compositions of composites for this type of SCA treatment are displayed. There is no significant change in the morphology of matrix when compared with non-treated ones. It was seen that weakly adhered serpentine particles were drawn from their embedded places upon fracture in Figure 3.4.a. However, a weak adhesion between filler and polymer was observed especially in Figure 3.6.a. We preferred to work on large size particles, although they appear seldom. Low resolution of the SEM device at high magnifications made it difficult to follow the presence of adhesion between polymer and filler through analysis of composites containing A-174 SCA. As shown in Figure 3.5.b and 3.6.a we hardly observe any strong adhesion.

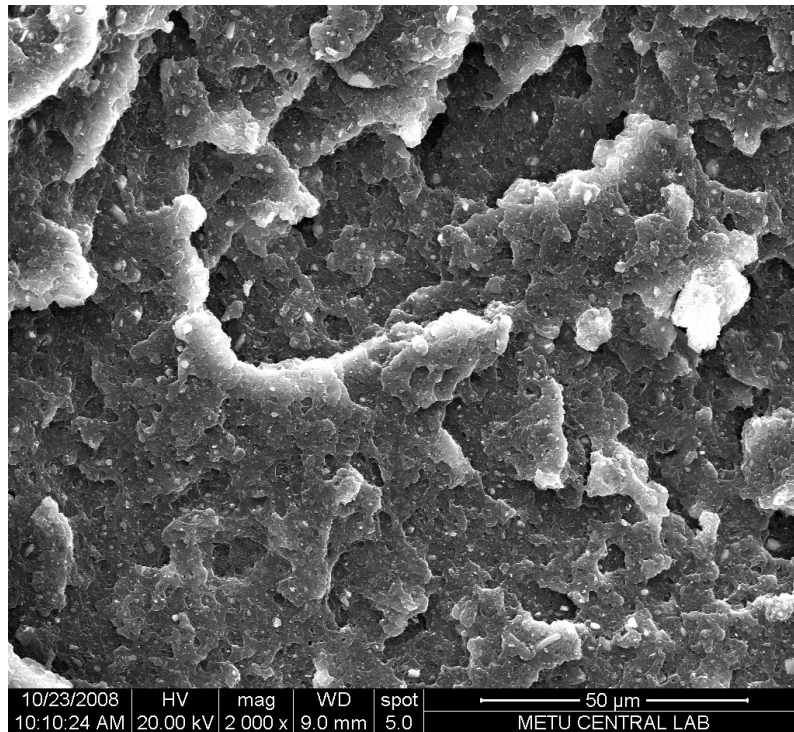
Figures 3.7, 3.8 and 3.9 show A-186 SCA treated serpentine filled composites. 2%, 5% and 10% addition of clay were monitored. Good chemical bonding and elevated interaction between serpentine and ABS was shown in Figure 3.7.b, Figure 3.8.b and Figure 3.8.c with high magnifications such as x10000 and x20000. In Figure 3.8.a, a large serpentine particle, which is almost fully contacted to polymer matrix was seen. It differs from other big particles by having almost no vacancy around it, interaction between serpentine and polymer was achieved. Closer views of this elevated interfacial interaction are given in Figure 3.8.b and 3.8.c.

5% and 10% A-189 SCA treated serpentine added composites were scanned and the images were given in Figure 3.10 and 3.11, respectively. A weak adhesion is observed similar to the one in A-174 treated composites. There are vacancies between the polymer and filler which can be clearly seen in Figure 3.11.

Additionally, it must be stated that fracture surfaces around bigger serpentine particles exhibited a more rough character compared to more homogeneously distributed sections of the specimen. Furthermore, little cavities, some containing a non-adhered serpentine particle and some being a cavity, were observed around those bigger serpentine particles. Micrographs explaining this morphology can be seen on Figure 3.2.b, Figure 3.5.b, Figure 3.6.a, Figure 3.8.a and Figure 3.10.b.

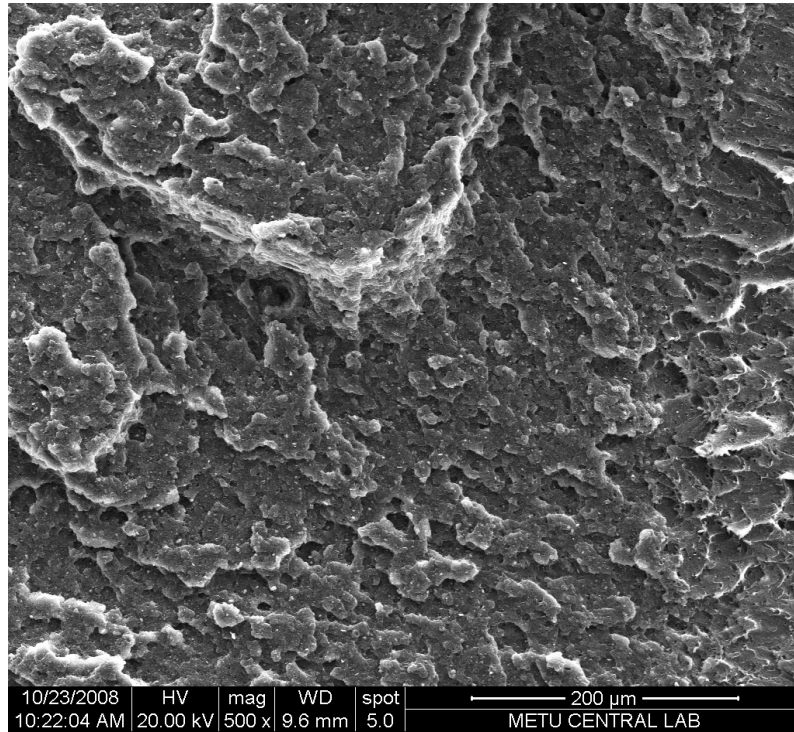


(a)

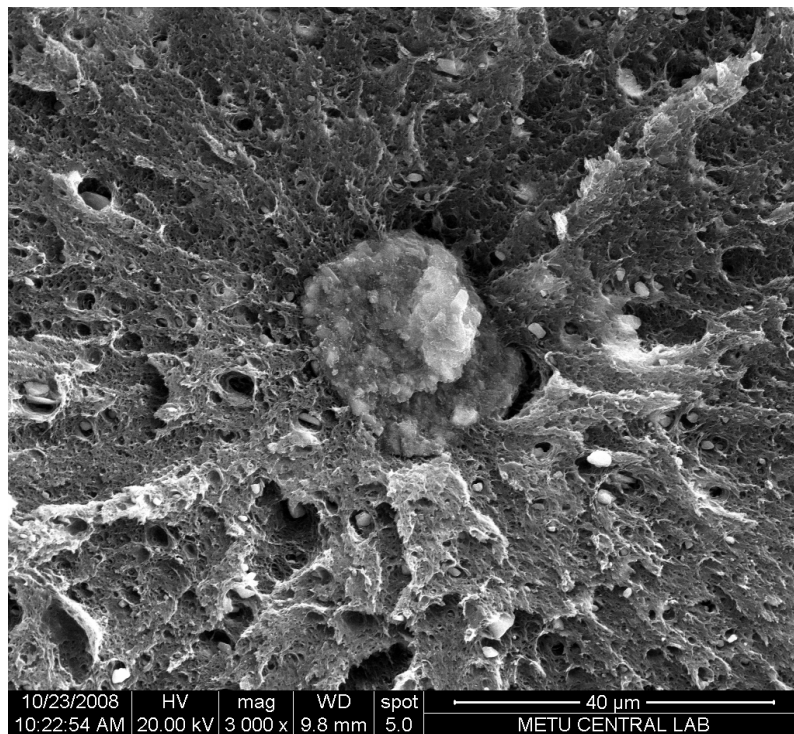


(b)

**Figure 3. 1** SEM image of fractured surface of ABS-5 (a) x2000–1 (b) x2000–2

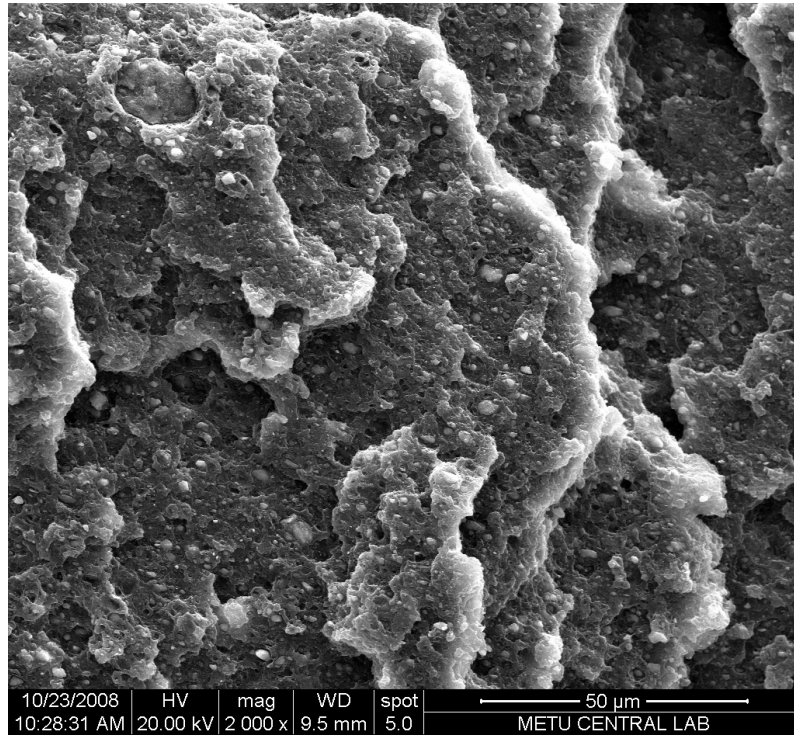


(a)

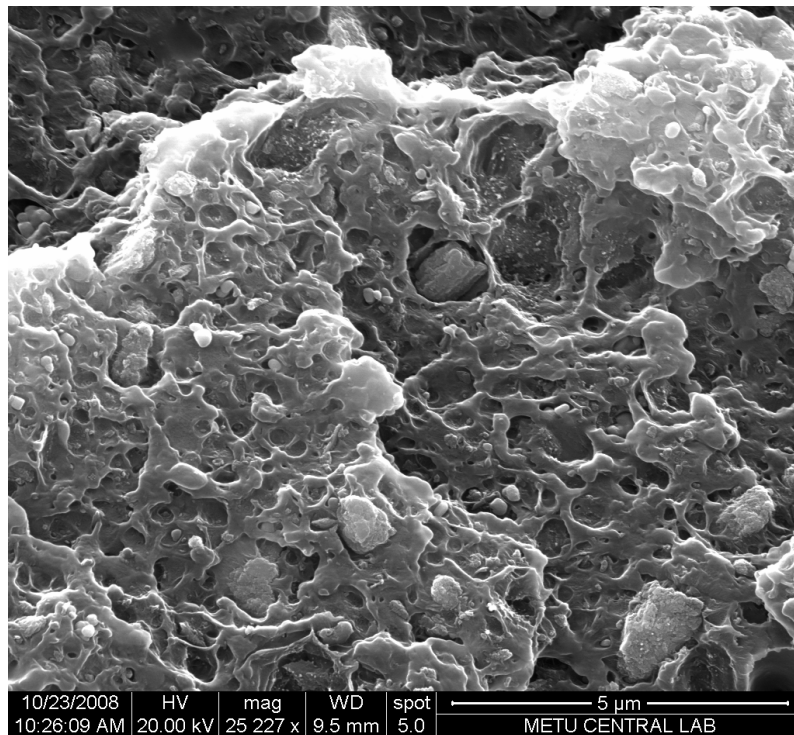


(b)

**Figure 3. 2** SEM image of fractured surface of ABS-10 (a) x500 (b) x3000

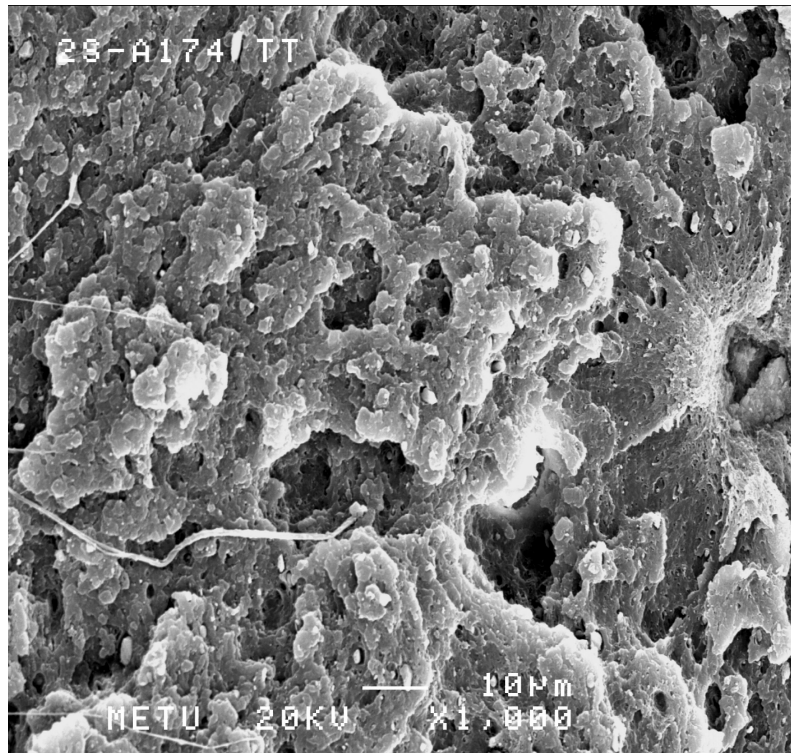


(a)

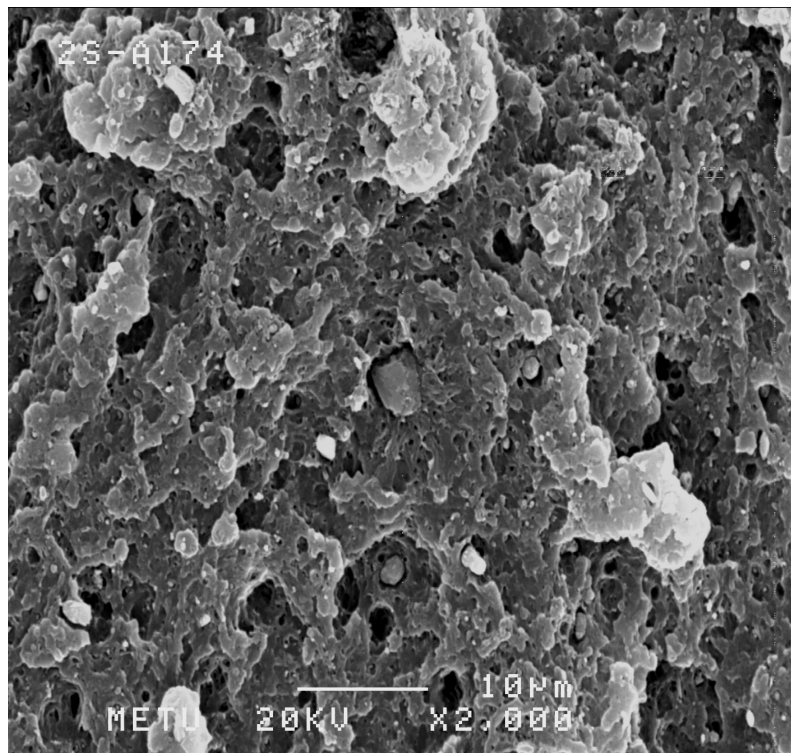


(b)

**Figure 3. 3** SEM image of fractured surface of ABS-20 (a) x2000 (b) x25227

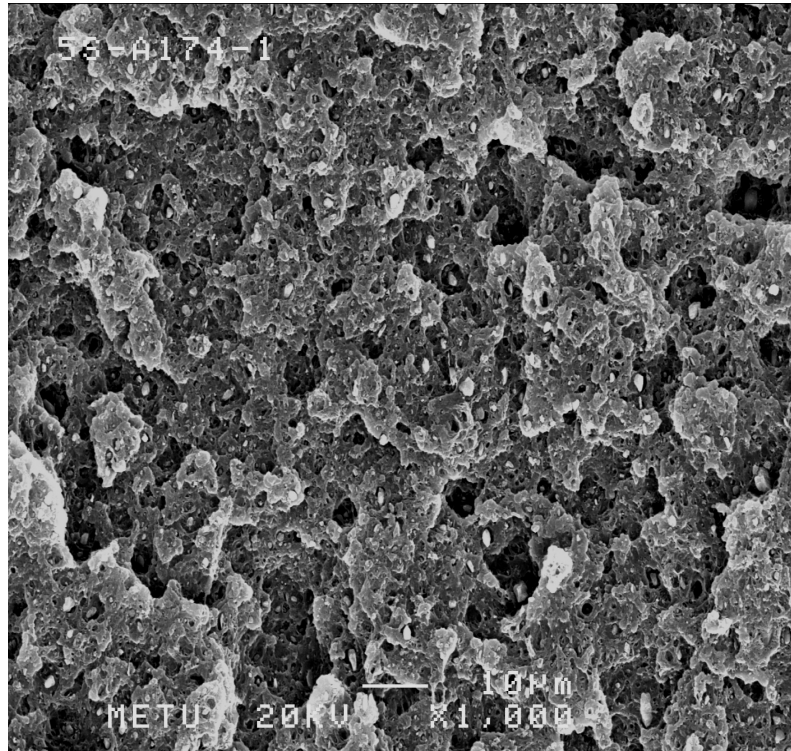


(a)

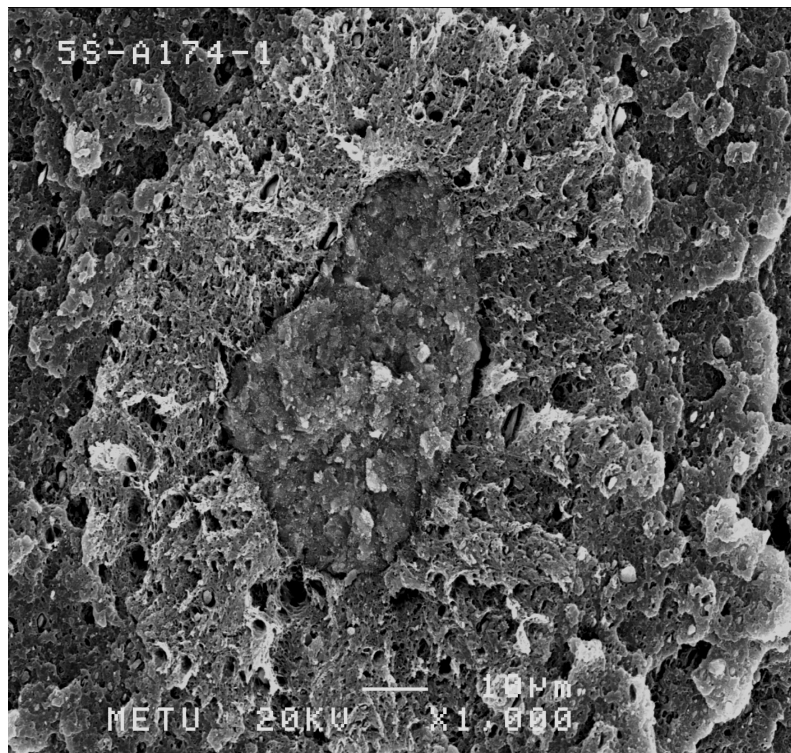


(b)

**Figure 3. 4** SEM image of fractured surface of ABS-2-174 (a) x1000 (b) x2000

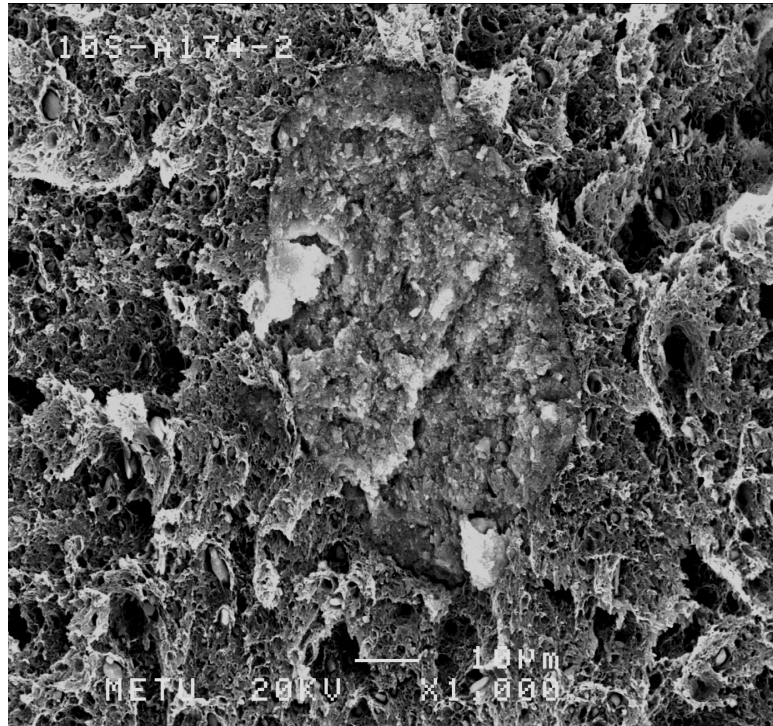


(a)

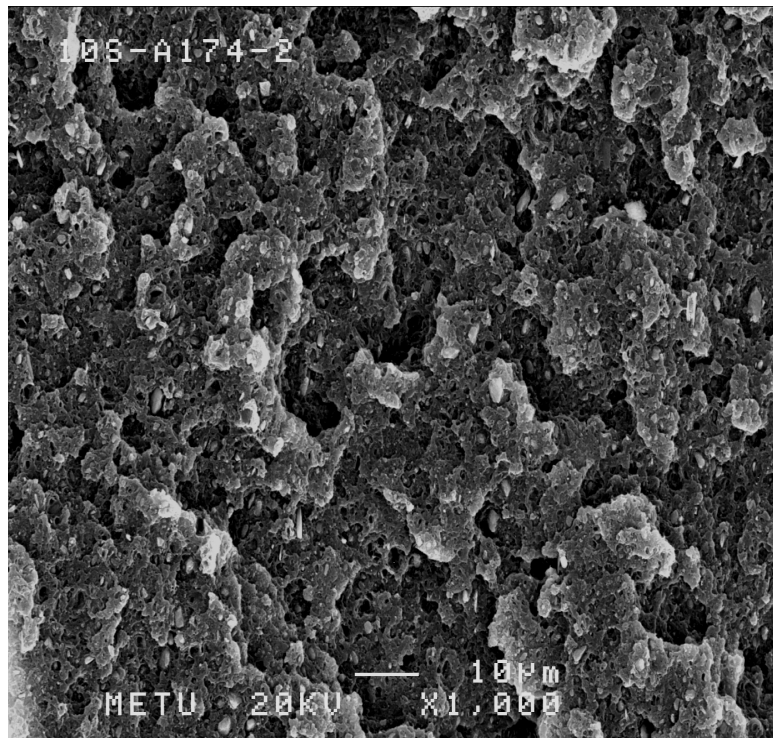


(b)

**Figure 3. 5** SEM image of fractured surface of ABS-5-174 (a) x1000-1 (b) x1000-2

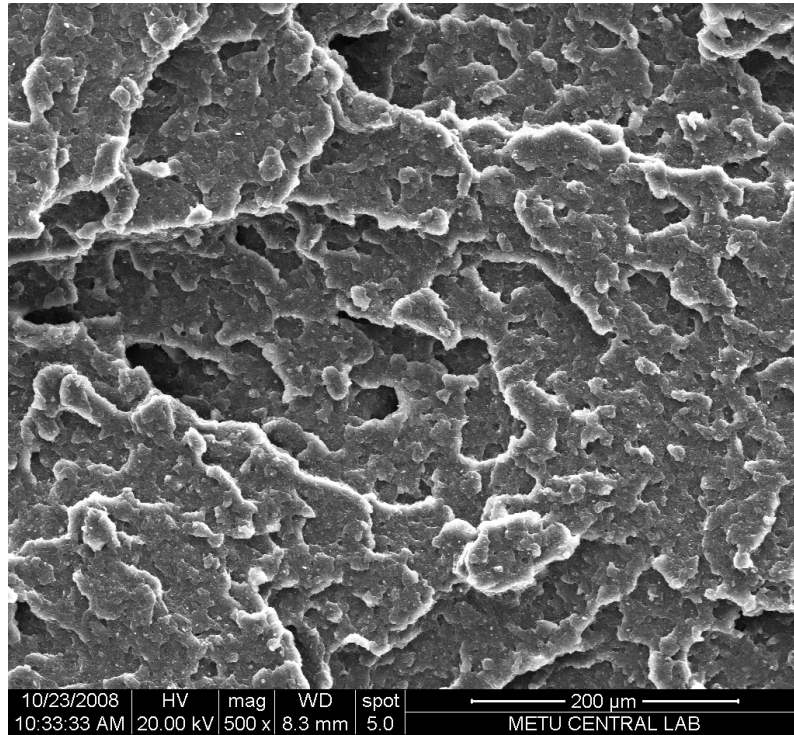


(a)

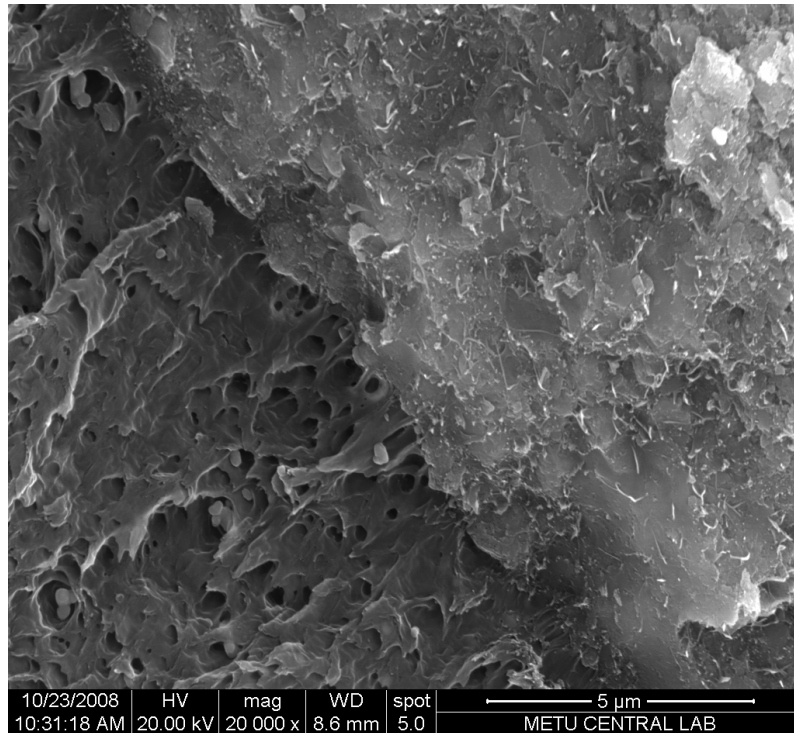


(b)

**Figure 3. 6** SEM image of fractured surface of ABS-10-174 (a) x1000-1  
(b) x1000-2

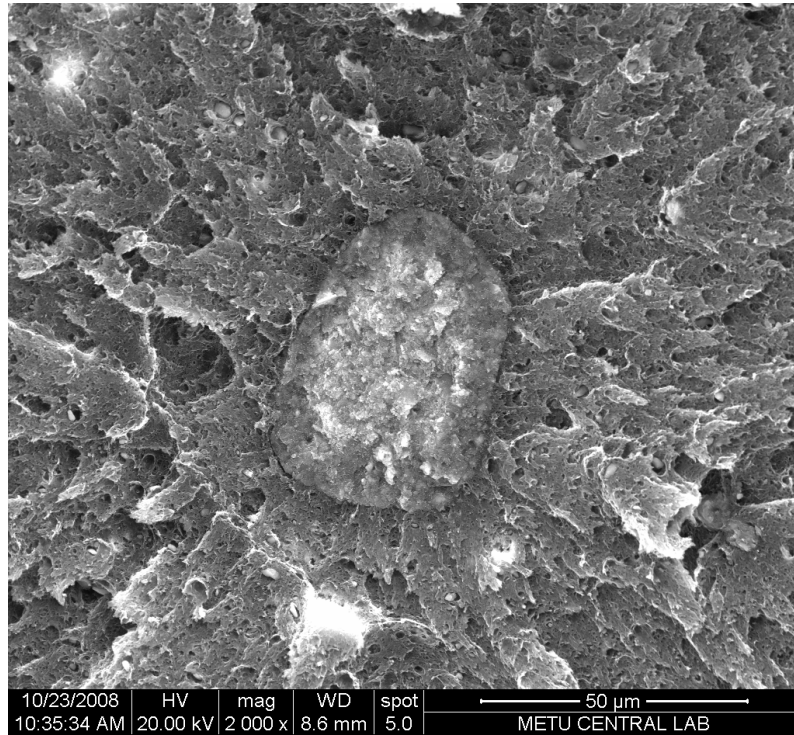


(a)

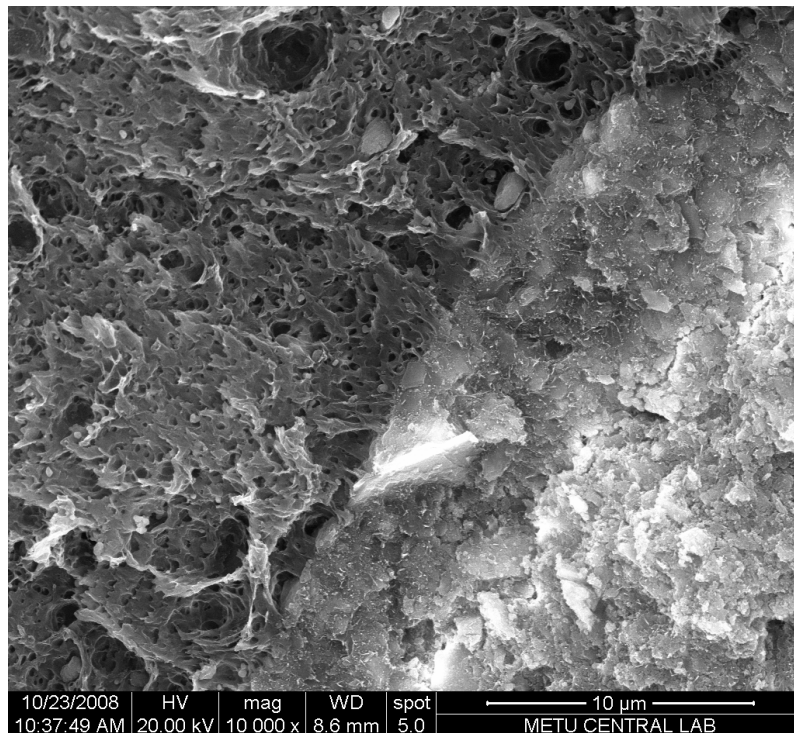


(b)

**Figure 3. 7** SEM image of fractured surface of ABS-2-186 (a) x500x (b) x20000

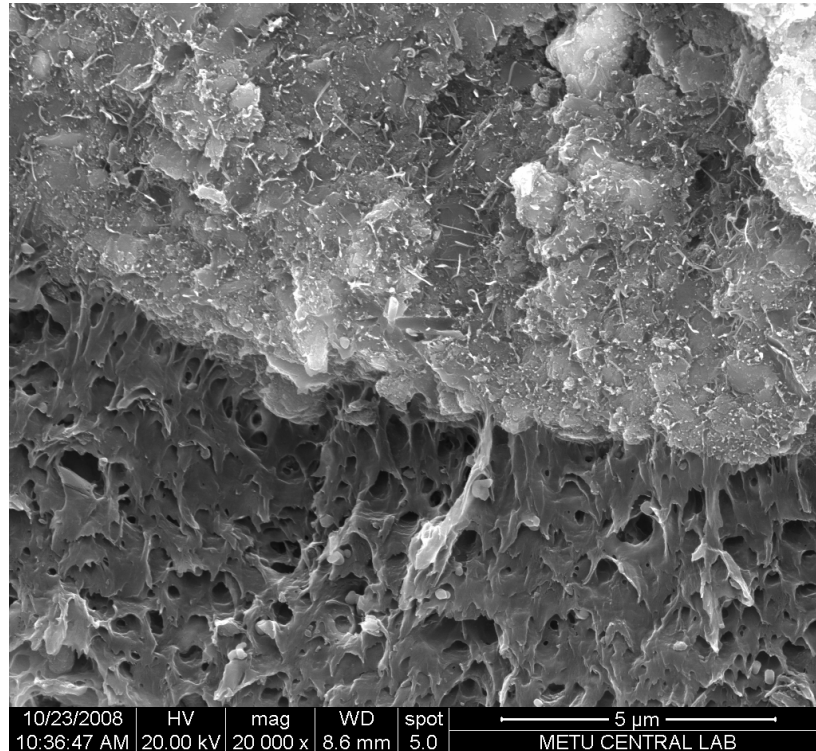


(a)



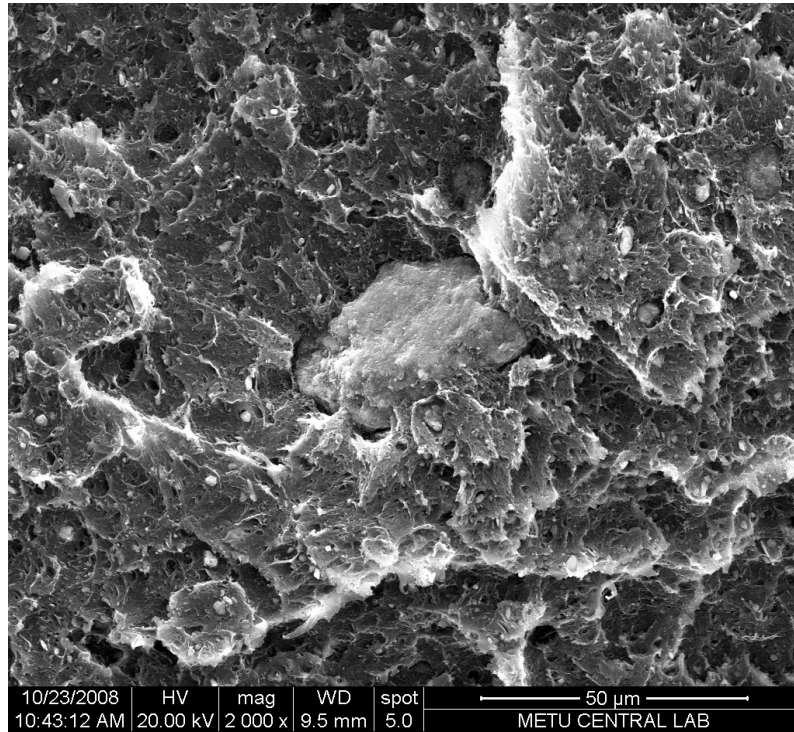
(b)

**Figure 3. 8** SEM image of fractured surface of ABS-5-186 (a) x2000 (b) x10000

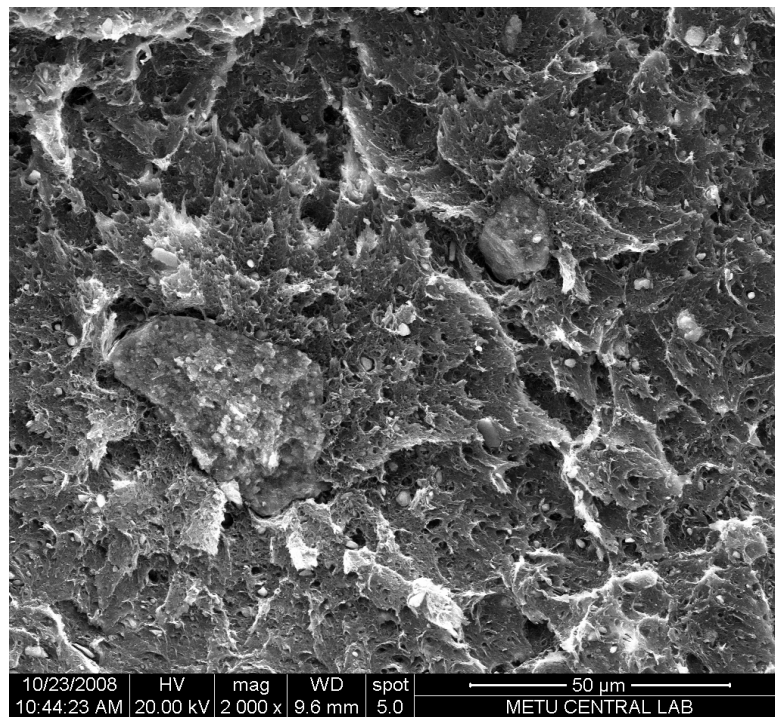


(c)

**Figure 3. 9** (cont'd) SEM image of fractured surface of ABS-5-186 (c) x20000

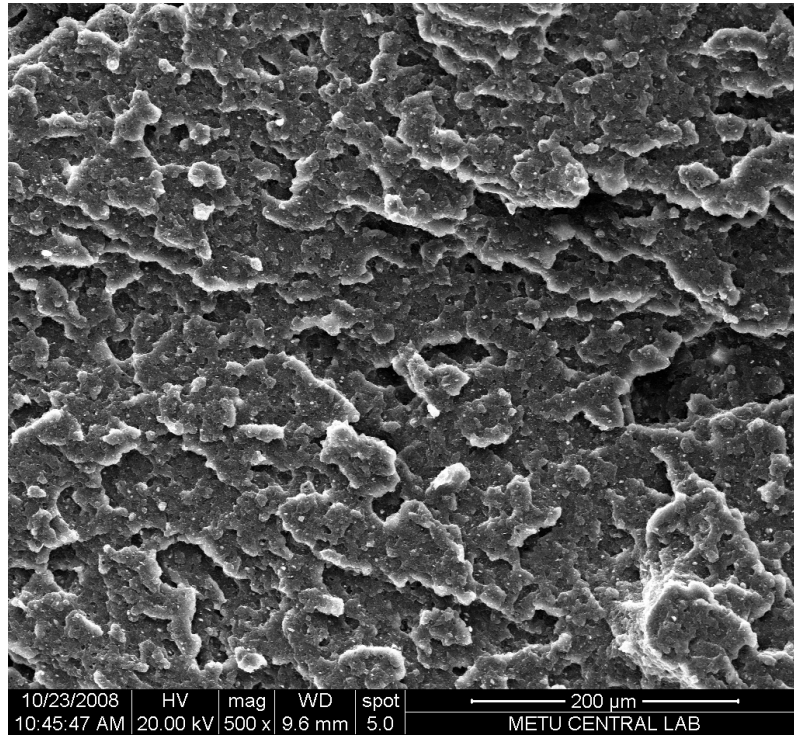


(a)

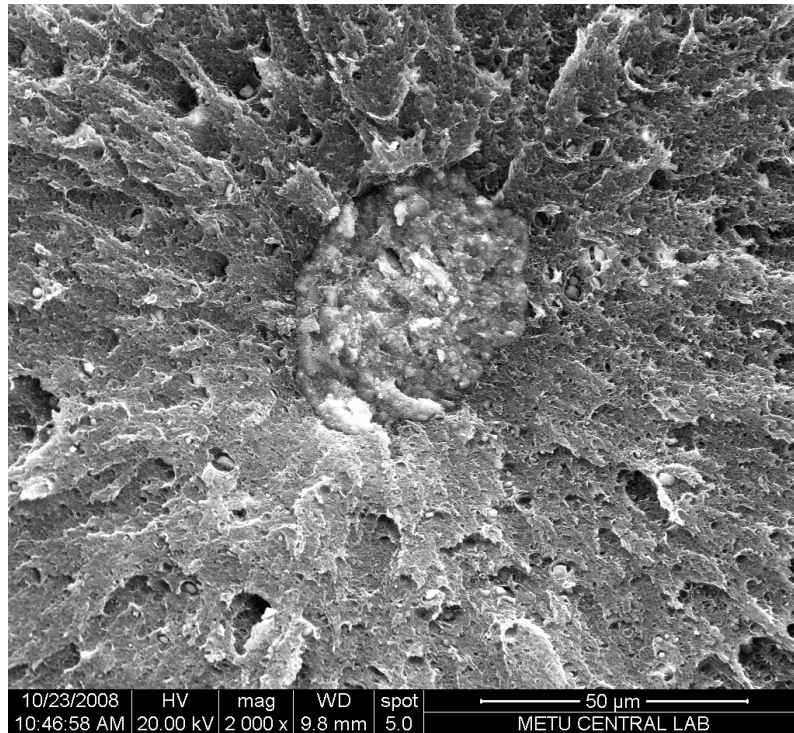


(b)

**Figure 3. 10** SEM image of fractured surface of ABS-10-186 (a) x2000–1  
(b) x2000–2

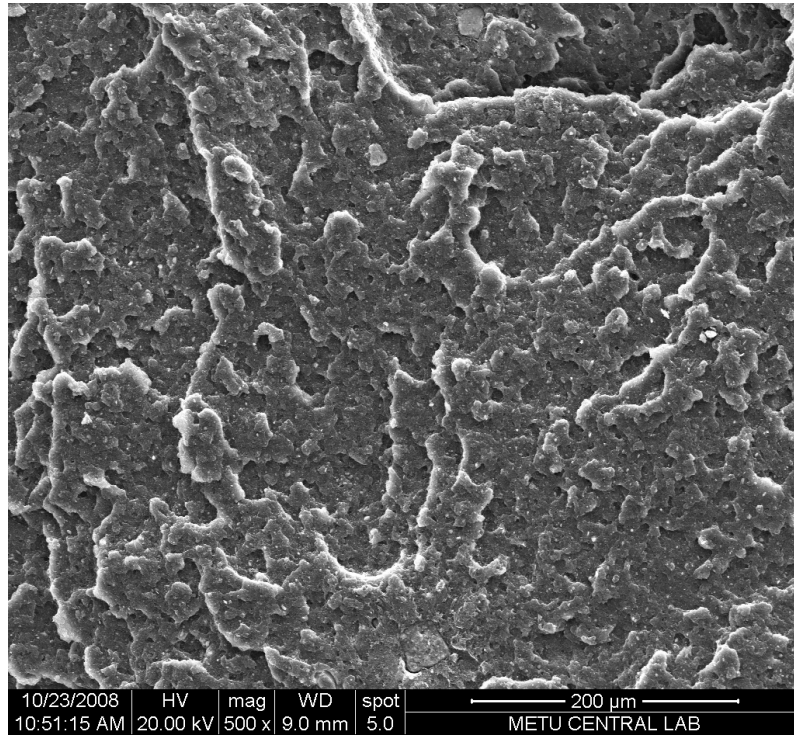


(a)

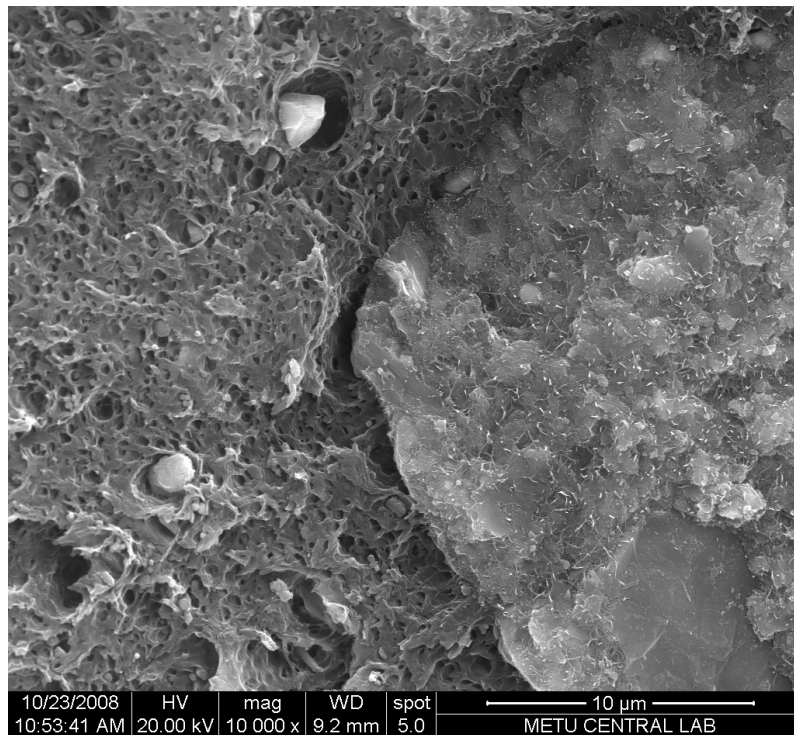


(b)

**Figure 3. 11** SEM image of fractured surface of ABS-5-189 (a) x500 (b) x2000



(a)



(b)

**Figure 3. 12** SEM image of fractured surface of ABS-10-189 (a) x500 (b) x10000

## **3.2. Mechanical Analysis**

Tensile testing and impact testing were applied to serpentine filled ABS composite to investigate the effects of filler, the order of addition of filler and SCA treatment to filler on mechanical properties. Results are graphically represented and all numerical data related to mechanical testing are given in Appendix A.

### **3.2.1. Tensile Testing**

Tensile testing was done on applied to injection molded dumbbell specimen to obtain information about resistance against one-directional stress and elongation response against this force. The data obtained from stress-strain diagrams were evaluated and characteristics of prepared composites were compared in terms of yield strength, elongation at break and Young's Modulus.

#### **3.2.1.1 Yield Strength and Elongation at Break**

Mineral type fillers are usually added to improve mechanical properties of polymers. Yield strength gives crucial information about mechanical properties because it is the measure of the force that a material can withstand before it suffers macroscopic plastic deformation. It is an important design parameter when choosing the right material for application.

The results of tensile testing are shown in Figures 3.12-3.17. First, the upper limit of addition of filler was determined by examining the point where mechanical properties have a critical change in a negative manner. 20% addition appeared to be the limiting point because all yield strength, elongation at break and impact strength (which will be discussed in the following section) properties exhibited a numerical loss. Elongation at break and impact strength losses were more significant ones.

The results for non-treated serpentine added fillers are shown in Figure 3.12 and the results of the SCA treated composites are shown in Figure 3.13, 3.14 and 3.15. From the yield strength point of view, there wasn't any loss up to 10% (including 10%) in all types of composites. Furthermore, 5% addition of serpentine gave the best results compared with 2% and 10% additions. SCA treatment has a positive effect towards yield strength properties. All of the SCA treated composites have greater yield strength values compared to non-treated ones. This was due to increased interface interaction between serpentine and ABS undoubtedly. As seen in Figure 3.14 and 3.16, ABS-5-186 had the greatest mechanical property improvement reaching to 12.9% advancement in yield strength value.

The elongation at break values of ABS was influenced with the filler addition. There was an increase in percent elongation values in 2% and 5% order of addition compared with maximum elongation of neat ABS which can be seen from Figure 3.12 to Figure 3.15 for individual sets and in Figure 3.17 for summary of all sets of composites. There was a slight increase in elongation at break values for ABS-10 and ABS-10-189 values but ABS-10-174 and ABS-10-186 had the same elongation at break values with respect to the neat ABS. As a result, none of the composites had a lower value compared to neat ABS. Three composites; ABS-2, ABS-10-174 and ABS-10-186 had nearly the same values and all of other composites have got a higher value compared to neat ABS. Abu Bakar et al. [35] suggested in their study with SCA treated kaolin/polypropylene composite that the increase in elongation at break value was due to the plasticizing effect of coupling agent. For 2% filler added composites, especially for ABS-2-189, this was true for serpentine/ABS composite. Furthermore, the lack of interaction between filler and coupling agent resulted with a failure in hindering the plastic deformation of the polymer matrix.

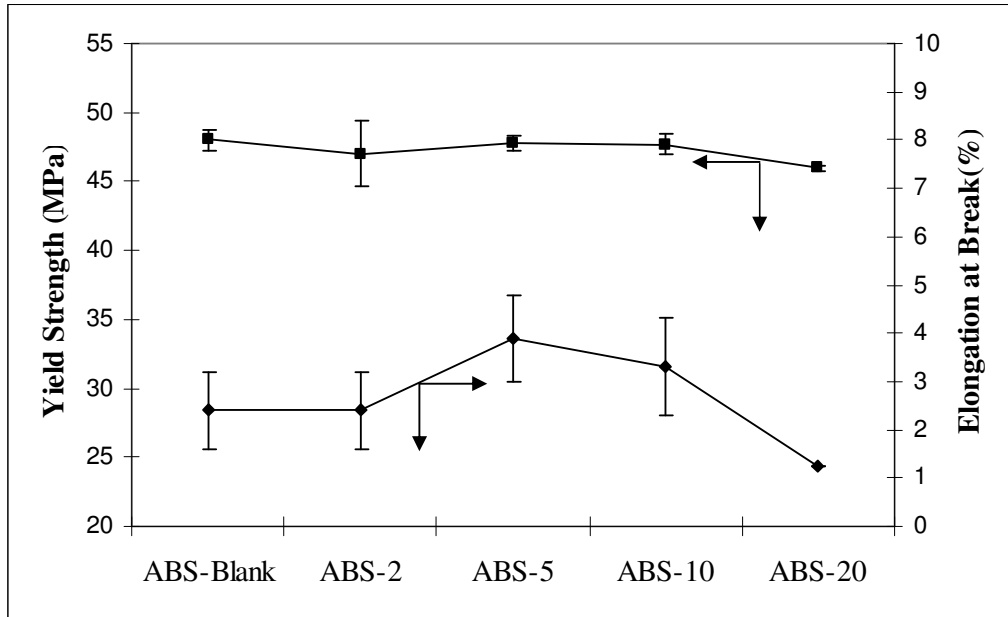


**Figure 3. 13** Yield Strength and Elongation at Break values for ABS composite

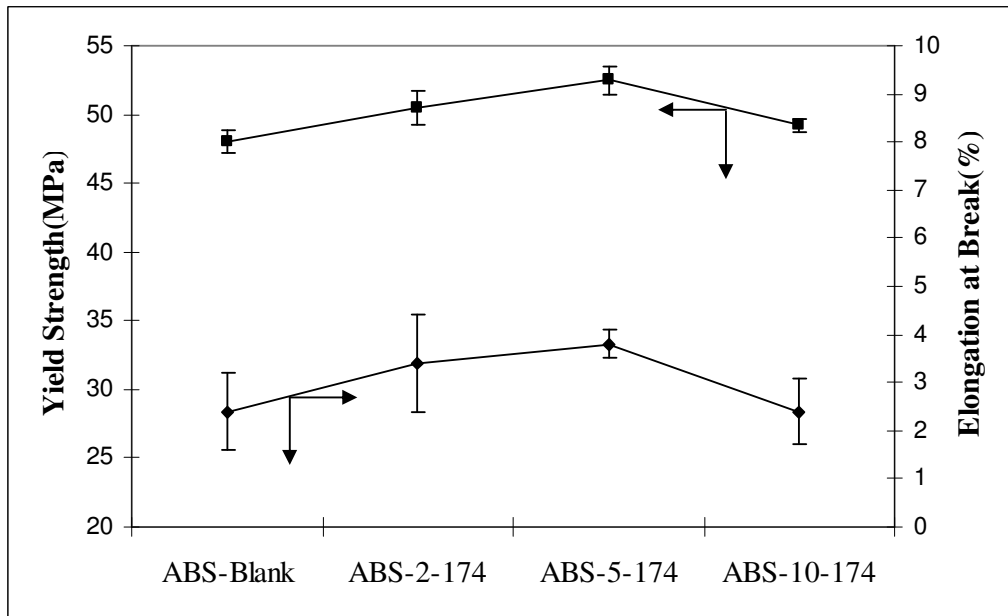


**Figure 3. 14** Yield Strength and Elongation at Break values for ABS-Blank and A-174 SCA treated serpentine filled ABS composite

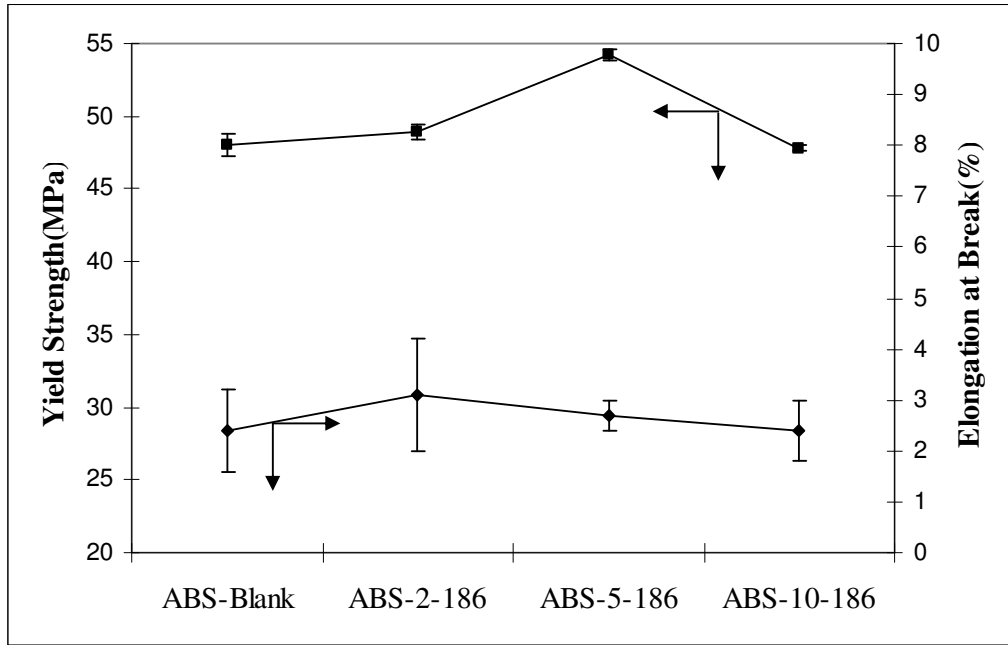


**Figure 3. 15** Yield Strength and Elongation at Break values for ABS-Blank and A-186 SCA treated serpentine filled ABS composite

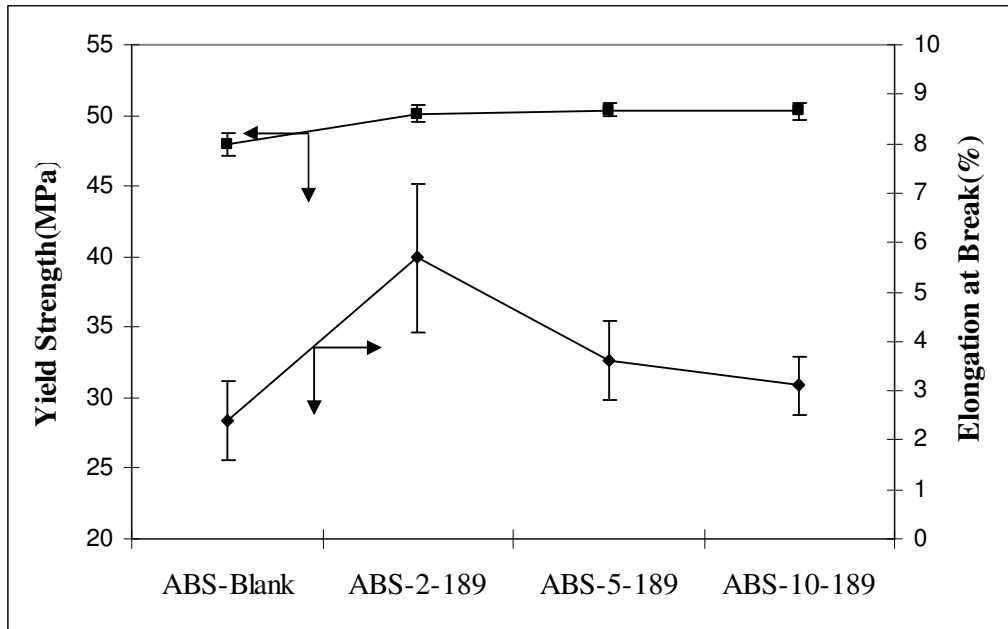


**Figure 3. 16** Yield Strength and Elongation at Break values for ABS-Blank and A-189 SCA treated serpentine filled ABS composite

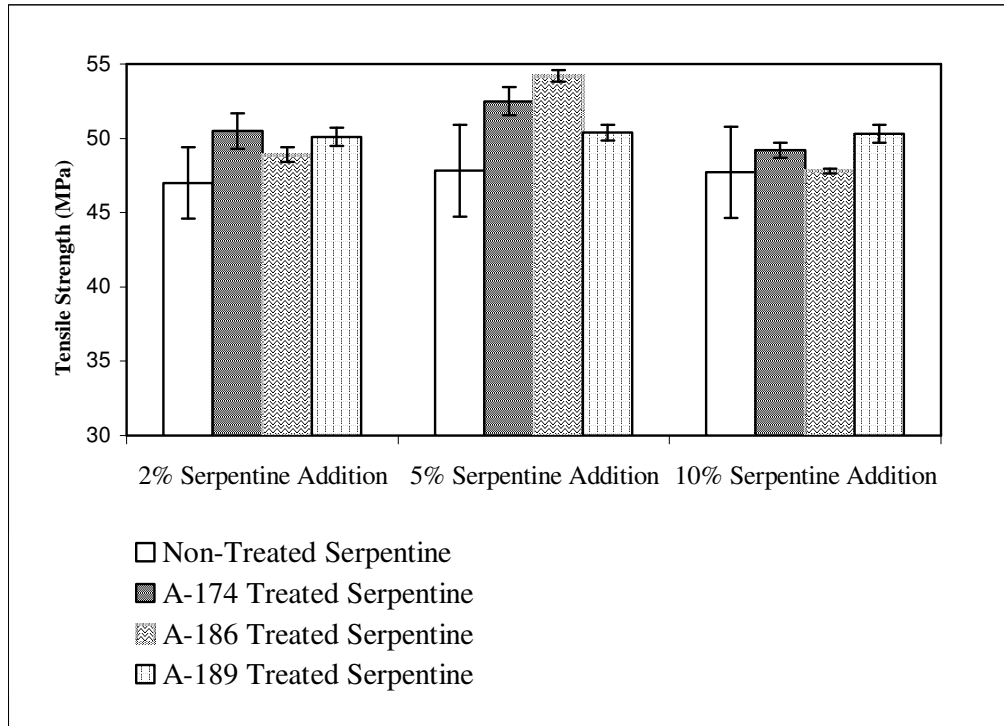


**Figure 3. 17** Comparison of Yield Strength values for all composites

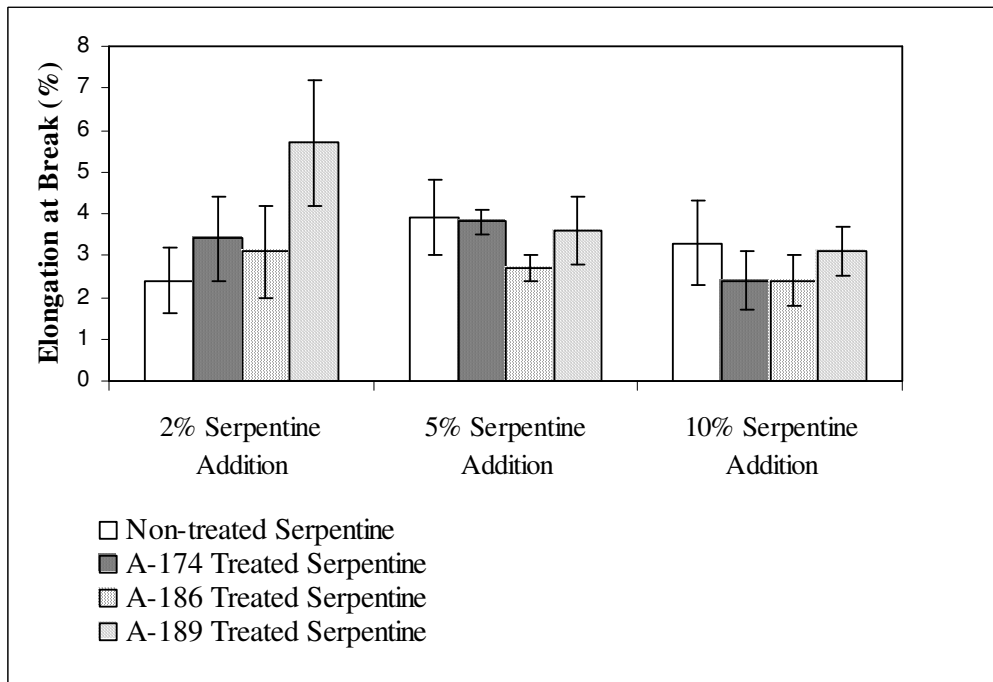


**Figure 3. 18** Comparison of Elongation at Break values for all composites

### 3.2.1.2 Young's Modulus

Young's modulus is the key indicator of the "stiffness" or "rigidity" which quantifies the resistance of the material to uniaxial tension [36]. Figure 3.18 compares the modulus of neat ABS, 2%, 5%, 10% and 20% serpentine filled ABS composites. A slight and linear increase in the modulus value up to 10% addition was observed but it decreased to a value near to neat-ABS for 20% addition. Second group of composites which were filled with A-174 SCA treated serpentine filled ABS exhibited a linear decrease response to increasing filler content which is shown in Figure 3.19. A-186 and A-189 treated serpentine filled ABS composites showed almost a constant response for modulus value to filler addition as depicted in Figure 3.20 and 3.21. Serpentine, which is a soft filler, but not as soft as talc, with its sticky and soapy feeling was apparently not very effective in altering the modulus of the matrix. Actually Kim et al. [37] found an interesting result, a decrease in modulus value in their study with a clay/polymer composite prepared with ABS/Cloisite 25A. Furthermore, in that study, the percent elongation at break was also found to be increasing up to 5 times of the neat ABS upon 3% and 5% SCA treated clay addition. where in our case we also observed enhancement in elongation at break values for most of the composites. Particularly for A-174 treated composites, the reduction in Young's modulus value should be the result of plasticizing effect of SCA.

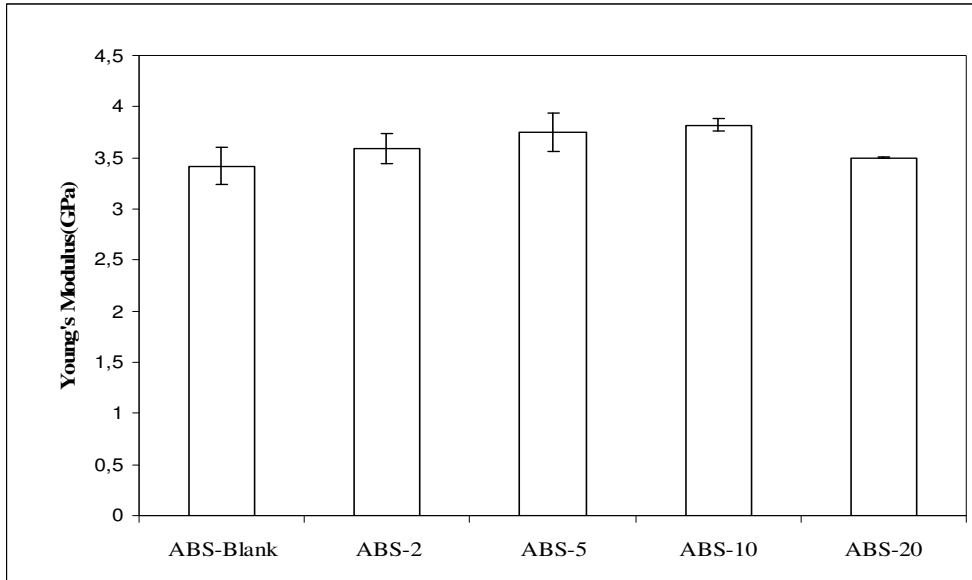


**Figure 3. 19** Comparison of Young's Modulus values of ABS-Blank, ABS-2, ABS-5, ABS-10 and ABS-20

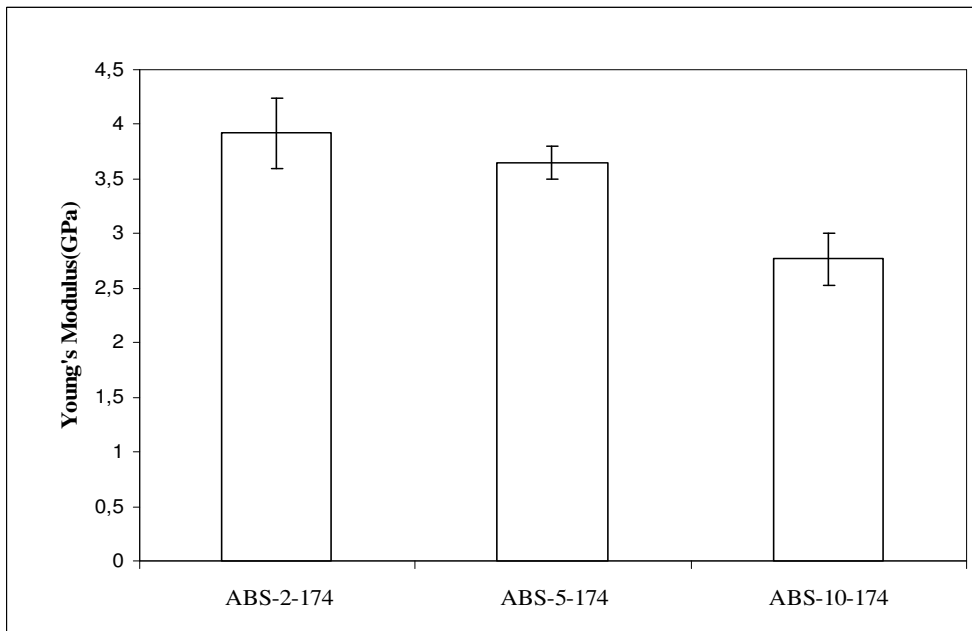


**Figure 3. 20** Comparison of Young's Modulus values of ABS-2-174, ABS-5-174 and ABS-10-174

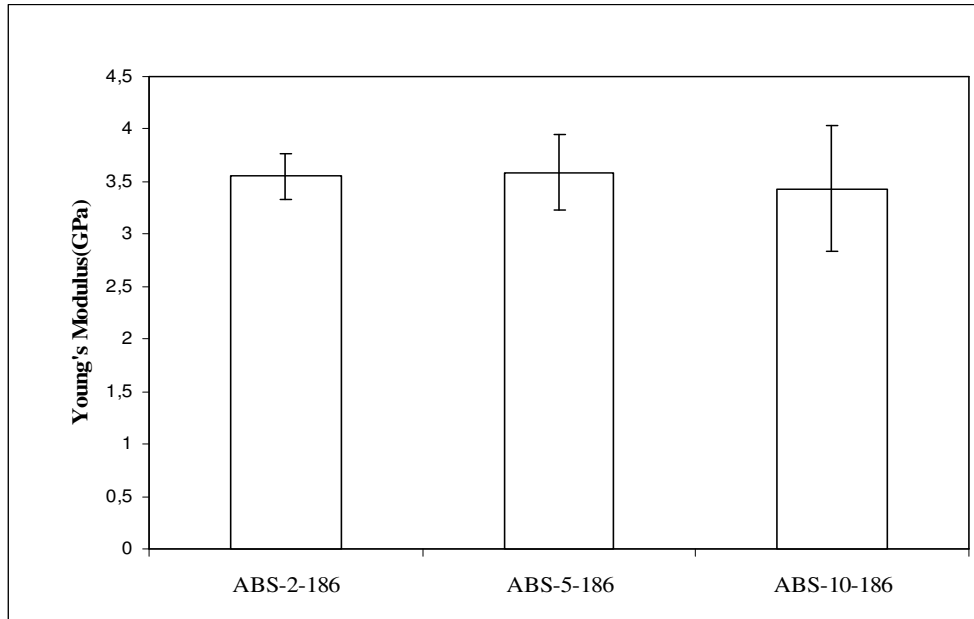


**Figure 3. 21** Comparison of Young's Modulus values of ABS-2-186, ABS-5-186 and ABS-10-186

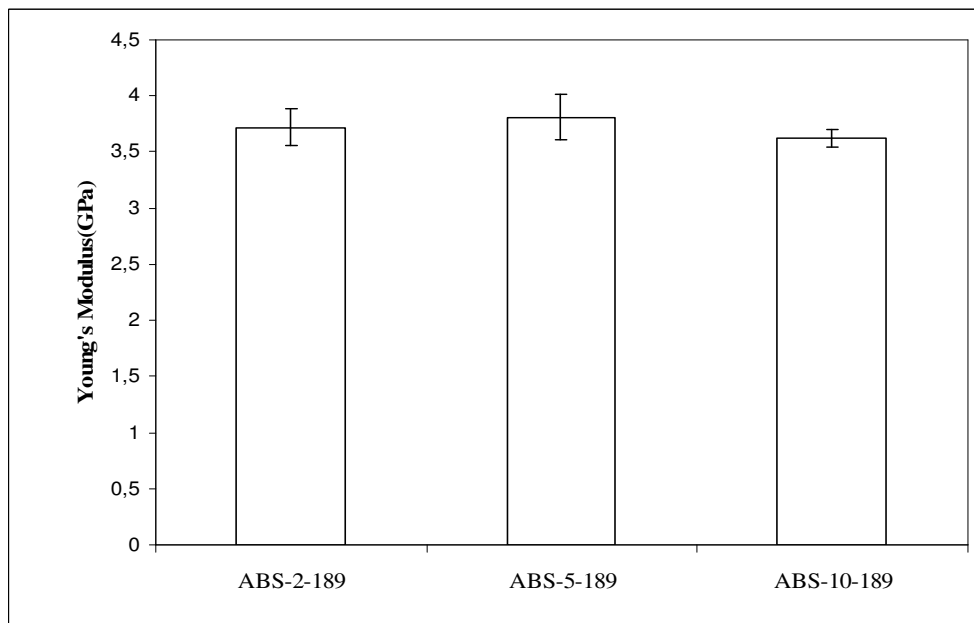


**Figure 3. 22** Comparison of Young's Modulus values of ABS-2-189, ABS-5-189 and ABS-10-189

### 3.2.2 Impact Testing

Impact testing provides information about toughness of the material. Unnotched and notched specimen are tested either by Izod Impact testing or Charpy Impact Testing, respectively. Charpy impact testing was applied to unnotched samples with a swinging pendulum and obtained data were in terms of energy loss per unit area as  $\text{kJ/m}^2$ . 4J pendulum was used for breaking samples however the equipment was insufficient to completely break samples having filler addition of 2%. Therefore, 2% filler added ABS regardless of SCA treatment maintained its toughness against impact forces. Data related with non-broken samples weren't included in the study.

The results were summarized in Figure 3.22. It was observed that increased addition of filler has reduced the toughness as expected since clay type fillers are known to convert ductile type of failure to brittle generally [7]. In this case, ABS already has some brittle character from the contribution of polystyrene, additionally, serpentine insertion boosted that property at 5% and after 5%. A dramatic decrease in impact strength occurred in 20% filler addition because of high concentration of serpentine particles. Lastly, results indicated that A-189 SCA treated serpentine filled composites showed the best impact strength values which agrees with percent elongation at break results. The greatest improvement in percent elongation values were obtained with A-189 treated composites which indicates that the area under the stress-strain diagram was also increased (taking into account that yield strength values were also increased) and toughness was increased. This could be due to the good wetting or dispersion effect of SCA. A-189 could have contributed the ease of particle dispersion of serpentine in ABS matrix. Better filler dispersion would have reduced the stress-concentration sites which are very sensitive to impact loading [35].

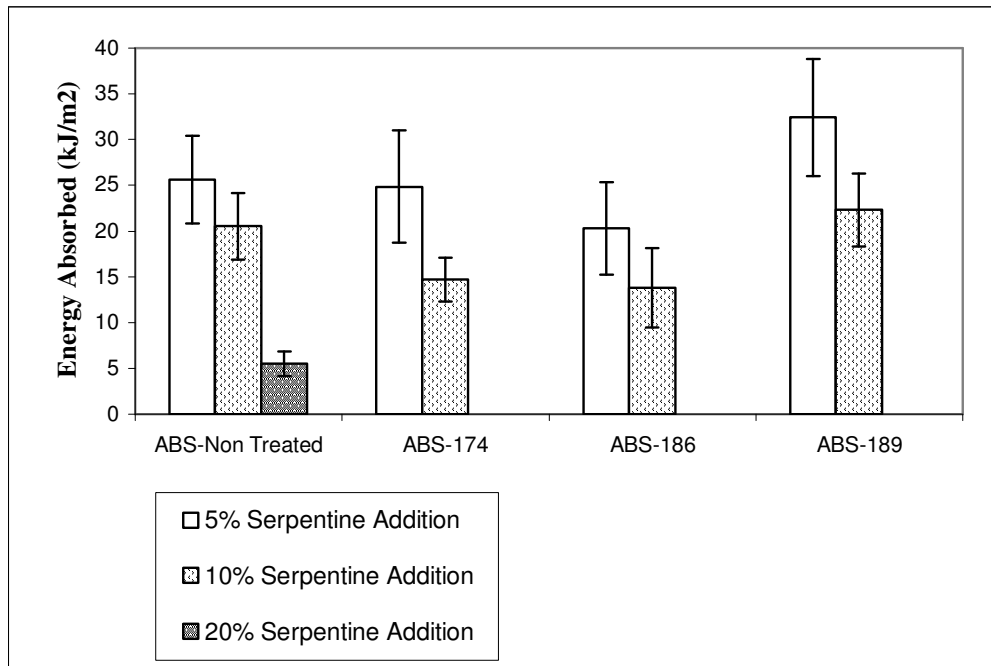


**Figure 3. 23** Impact Strength data of totally broken samples

### 3.3. Thermal Characterization by DSC Analysis

Thermal analysis was performed to observe the effects of nontreated filler and SCA treated filler contribution on thermal property, mainly on glass transition temperature ( $T_g$ ). DSC thermograms of the composites are given in Appendix B and Table 3.1 lists the  $T_g$  values of neat ABS and composites. It can be concluded that there is an average difference in  $T_g$  values between neat ABS and serpentine filled ABS such as 4 - 4,5°C. 12 out of 13 samples have lower glass transitions compared with neat ABS. Stiffness of the chains are somewhat decreased by introduction of the serpentine particles weakly adhered to the polymer matrix and much freedom for motion of chain segments were created. [36] It seems that A-189 treated serpentine filled ABS composites gained the biggest free volume according to these results because they have the greatest decrease in  $T_g$  values, 6,5°C in average, with respect to neat ABS. In addition, this decrease in  $T_g$  values, particularly seen in SCA treated composites, could be the result of plasticizing effect of the coupling agents.

**Table 3. 1** T<sub>g</sub> values derived from DSC thermograms

Sample Code	T <sub>g</sub> (°C)	Sample Code	T <sub>g</sub> (°C)
ABS-Blank	108.5	ABS-10-174	101.9
ABS-2	105.6	ABS-2-186	104.5
ABS-5	106.6	ABS-5-186	103.0
ABS-10	109.1	ABS-10-186	104.8
ABS-20	104.6	ABS-2-189	101.8
ABS-2-174	104.0	ABS-5-189	101.7
ABS-5-174	103.3	ABS-10-189	102.0

### 3.4. Flow Characteristics Determination by Melt Flow Index (MFI) Analysis

MFI is a measure of the ease of flow of a thermoplastic polymer. The mass of molten polymer flowing through a capillary under a pressure maintained with a defined mass for a certain period of time gives MFI value of the sample. In this study, all the measurements were done with a load of 2.16 kg and 10 minutes sampling time were done for all samples. Table 3.2 gives the results of the MFI measurements.

**Table 3. 2** MFI results of all samples

Sample Code	MFI Value (g/10 min)	Sample Code	MFI Value (g/10 min)
<b>ABS-Blank</b>	3.63 (± 0.06)	<b>ABS-5-174</b>	2.58 (± 0.10)
<b>ABS-2</b>	3.58 (± 0.05)	<b>ABS-10-174</b>	1.71 (± 0.06)
<b>ABS-5</b>	3.14 (± 0.05)	<b>ABS-2-186</b>	3.78 (± 0.11)
<b>ABS-10</b>	2.81 (± 0.05)	<b>ABS-5-186</b>	3.17 (± 0.02)
<b>ABS-20</b>	1.42 (± 0.07)	<b>ABS-10-186</b>	2.23 (± 0.04)
<b>ABS-2-174</b>	3.81 (± 0.04)	<b>ABS-2-189</b>	3.71 (± 0.04)
<b>ABS-5-189</b>	3.07 (± 0.0)	<b>ABS-10-189</b>	2.44 (± 0.09)

The MFI values show that at 2% addition of serpentine with SCA treatment, viscosities were slightly decreased compared to neat ABS which suggests that for 2% SCA treated serpentine filled composites, surface modification of serpentine was achieved and plasticizing effect of SCA was observed [38]. For ABS-2, the MFI value was very close to that of ABS-Blank. However, as expected, addition of serpentine more than 2% to ABS ( which was defined as high flow type by producer) decreased the MFI values or increased the viscosity. This was because of hindering effect of serpentine particles and possible agglomerates to the flow of the composite. As the filler content increased, MFI value was further decreased. Viscosity of SCA treated serpentine filled composites also increased when filler addition was increased. There was not any significant difference between MFI values for different types of SCA. A representative figure for the melt flow characteristics of ABS/serpentine composite is given in Figure 3.23

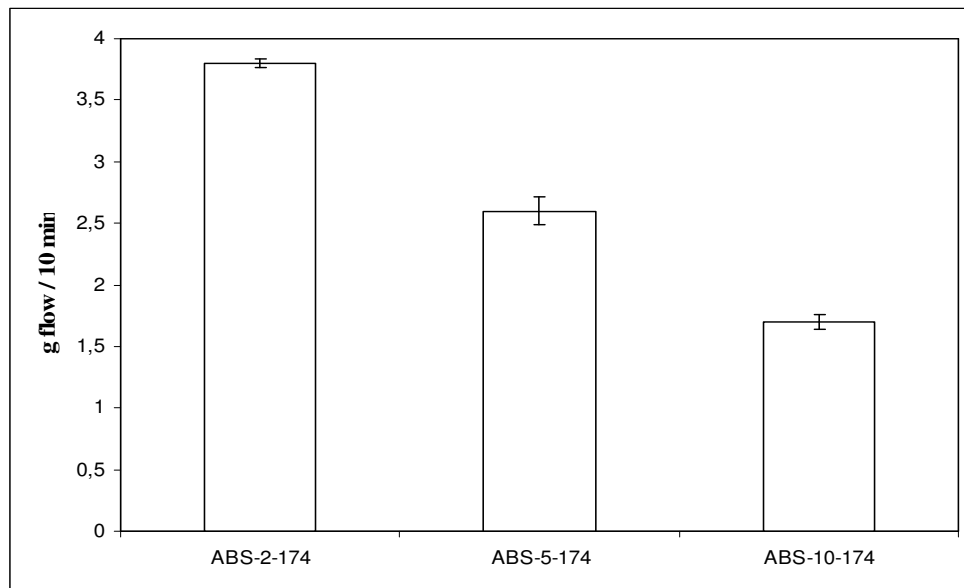


**Figure 3. 24** MFI for A-174 SCA treated serpentine filled ABS composite

## CHAPTER 4

### CONCLUSIONS

Morphological analyses were done with SEM. It was found that distribution of the filler serpentine through ABS matrix was homogeneous. The interaction on polymer-filler interface was examined and it was determined that there was a very weak interaction between non-treated serpentine and polymer. However with SCA treatment an improvement in the adhesion was observed especially in samples treated with A-186 SCA. Rough fracture surfaces were determined around bigger serpentine particles compared to surface around average serpentine particles.

Mechanical tests were performed in order to characterize tensile and properties. Yield strength, percent elongation at break and Young's Modulus values were investigated in tensile testing part. There was not any dramatic mechanical property loss up to 20% of filler addition. SCA treated samples gave the best results for yield strength property because of altered interface interaction. ABS-5-186 had shown 12.9% improvement in yield strength value with respect to neat ABS. The percent elongation at break values were increased after filler addition whether SCA treatment was applied or not. ABS-2-189 composite had a percent elongation at break value nearly 2.5 times higher than neat ABS which could be the plasticizing effect of SCA. Serpentine addition did not change the Young's Modulus values significantly. The most interesting results were taken from ABS-20 and A-174 SCA treated samples, such that they had a decrease in Young's Modulus value with filler addition. This ineffectiveness in improvement in elastic modulus value was possibly due to the softness of serpentine with its sticky and soapy feeling.

In unnotched Charpy impact testing, 2% serpentine filled composites were not broken with the equipment like the neat ABS. It can be concluded that up to 2%

addition, no dramatic decrease occurred. However starting from 5% of addition, toughness of the ABS could not be maintained and in 20% addition, the decrease was significant. Best results for impact testing were obtained from A-189 SCA treated composites, which had the greatest percent elongation improvement through all composites.

Thermal analysis showed that the glass transitions of composites were decreased by 4-4.5°C in average upon filler addition. The greatest decrease in  $T_g$  was observed for A-189 SCA treated samples as 6.5°C in average. This was probably because of a decrease in chain stiffness. For SCA treated composites, it could be the plasticizing effect of the coupling agents that created a larger difference in  $T_g$  values compared to  $T_g$  values of non-treated composites.

MFI analyses have shown that 2% addition of serpentine did not affect the flow properties of composite negatively compared to neat ABS. In addition, for 2% filler addition, all MFI values of SCA treated composites have found to be larger than neat ABS. This could be the result of surface modification of composites with SCA treatment. However, the viscosities of all composites, regardless of SCA treatment, were increased significantly with filler addition over 2%. This was due to hindering effect of serpentine particles to the flow.

## REFERENCES

1. A.B. Strong, "High Performance and Engineering Thermoplastic Composites", Technomic Publishing Company Inc., USA, (1993)
2. R.M. Jones, "Mechanics of Composite Materials", Taylor and Francis Inc., USA, (1999)
3. D. Gay, S.V. Hoa, S.W. Tsai, "Composite Materials: Design and Application, CRC Press, USA, (2003)
4. B.Z. Jang, Advanced Polymer Composites: Principles and Applications, ASM International, USA, (1996)
5. S.K. Mazumdar, "Composites Manufacturing Materials, Product and Process Engineering", CRC Press LLC, US, (2002)
6. M. Xanthos, Functional fillers for plastics, Wiley-VCH Verlag GmBH&Co., Weinheim, Germany, (2005)
7. R.N. Rethon, (Ed.), Particulate-Filled Polymer Composites, Rapra Technology Limited, Shrewsbury, (2003)
8. W.B. Jepson, Philosophical Transactions Royal Society London, (1984) (A comprehensive, brief review of kaolinn, its occurrence, properties and production)
9. G. Wypych, Handbook of Fillers, ChemTec Publ., Toronto, Canada, (2000)

10. A.V. Milovsky, O.V. Kononov, Mineralogy, Mir Publishers, Moscow, (1982)
11. C. Klein, C.S. Hurlbut, Jr., Manual of Mineralogy, John Wiley and Sons Inc., USA, (1993)
12. M.H. Battey, Mineralogy For Students, Hafner Press, New York, USA, (1982)
13. (Plastics Industry Producers Statistics Group Resin Statistics Summary 2007 vs. 2006, American Chemistry Council)
14. C.H. Basdekis, ABS Plastics, Reinhold Publishing Corporation, New York, USA, (1954)
15. M. Chanda, S.K. Roy, Plastics Technology Handbook, CRC Press LLC, US, (2007)
16. J.A. Brydson, Plastics Materials, Butterworth Heinemann, Oxford, UK, (1999)
17. H.F. Mark, Encyclopedia of Polymer Science and Technology, John Wiley&Sons Inc., USA, (2005)
18. P.N. Prasad, J.E. Mark, T.J. Fai(Ed.), Polymers and Other Advanced Materials, Plenum Press, New York, USA, (1995)
19. L.A. Utracki, Commercial Polymer Blends, Champan and Hall, UK, (1998)
20. L. Jiang, Y.C. Lam, K.C. Tam, T.H. Chua, G.W. Sim, L.S. Ang, Polymer, Vol. 46, Issue 1, p.243-252, (2005)

21. G. Lu, X. Li, H. Jiang, Composites Science and Technology, Volume 56, Issue 2, p.193-200, (1999)
22. S.S. Tzeng, F.Y. Chang, Mater. Sci. and Eng, Vol. 37, p. 258-267, (2001)
23. J.Z. Liang, Journal of Elastomers and Plastics, Vol. 37, p.361-360, (2005)
24. S.C. Tjong, W. Jiang, Journal of Applied Polymer Science, Vol. 73 p.2985-2991(1999)
25. H.Ö. Gülsoy, M. Taşdemir, Polymer-Plastics Technology and Engineering, Vol. 46, p. 789-793, (2007)
26. J. Kim, K. Lee, L. Kunwoo, J. Bae, J. Yang, S. Hong, Polymer Degradation and Stability, Vol. 79, p. 201-207, (2003)
27. B. Liu, Y. Zhang, C. Wan, R. Li, B. Liu, Polymer Bulletin, Vol. 58, p. 747-755, (2007)
28. S. Wang, Y. Hu, L. Song, Z. Wang, Z. Chen, W. Fan, Polymer Degradation and Stability, Vol. 77, p. 423-426, (2002)
29. S. Wang, Y. Hu, Z. Lin, , Z. Wang, Z. Gui, Z. Chen, W. Fan, Polymer International, Vol. 52, p. 1045-1049, (2003)
30. S. Wang, Y. Hu, L. Zong, Y. Tang, Z. Chen, W. Fan, Applied Clay Science, Vol. 25, p.49-55, (2004)
31. H. Ma, Z. Xu, L. Tong, A. Gu, Z. Fang, Polymer Degradation and Stability, Vol. 91, p. 2951-2959, (2006)

32. A.P. Patino-Soto, S. Sanchez-Valdez, L.F. Romos-de Valle, Journal of Polymer Science Part B:Polymer Physics, Vol. 46, Issue 2, p.190-200,(2008)
33. Y.S. Choi, M. Xu, I.J. Chung, Polymer, Vol. 46, p. 531-538, (2005)
34. S. Tan, Ph. D. Thesis of the Department of Polymer Science and Technology, The Graduate School of Natural and Applied Sciences of METU (2008)
35. M.B. Abu Bakar, Y.W. Leong, A. Ariffin, Z.A. Mohd Ishak, Journal of Applied Polymer Science, Vol. 110, p.2770-2779, (2008)
36. J. Bicerano, Prediction of Polymer Properties, Marcel Dekker Inc., New York, USA (1993)
37. H.S. Kim, B.Y. Park, J.H. Choi, J.S. Yoon, Journal of Applied Polymer Science, Vol. 107, p. 2539–2544 (2008)
38. C.D. Han, T. Van Den Weghe, P. Shete, J.R. Haw, Polymer Engineering and Science, Vol. 21, Issue 4, p.196-204 (1981)

## APPENDIX A

### TENSILE PROPERTIES DATA

**Table A. 1** Average Yield Strength and Percent Elongation at Break Values for Composites

<b>Sample</b>	<b><math>\sigma</math> (MPa)</b>	<b><math>\epsilon</math> (%)</b>
<b>ABS-Blank</b>	48.0 ( $\pm 0.8$ )	2.4( $\pm 0.8$ )
<b>ABS-2</b>	47.0 ( $\pm 2.4$ )	2.4( $\pm 0.8$ )
<b>ABS-5</b>	47.8( $\pm 0.5$ )	3.9( $\pm 0.9$ )
<b>ABS-10</b>	47.7( $\pm 0.7$ )	3.3( $\pm 1.0$ )
<b>ABS-20</b>	46.0 ( $\pm 0.2$ )	1.25( $\pm 0$ )
<b>ABS-2-174</b>	50.5( $\pm 1.2$ )	3.4( $\pm 1.0$ )
<b>ABS-5-174</b>	52.5( $\pm 1.0$ )	3.8( $\pm 0.3$ )
<b>ABS-10-174</b>	49.2( $\pm 0.5$ )	2.4( $\pm 0.7$ )
<b>ABS-2-186</b>	48.9( $\pm 0.5$ )	3.1( $\pm 1.1$ )
<b>ABS-5-186</b>	54.2( $\pm 0.4$ )	2.7( $\pm 0.3$ )
<b>ABS-10-186</b>	47.8( $\pm 0.2$ )	2.4( $\pm 0.6$ )
<b>ABS-2-189</b>	50.1( $\pm 0.6$ )	5.7( $\pm 1.5$ )
<b>ABS-5-189</b>	50.4( $\pm 0.5$ )	3.6( $\pm 0.8$ )
<b>ABS-10-189</b>	50.3( $\pm 0.6$ )	3.1( $\pm 0.6$ )

**Table A. 2** Young's Modulus Values for Composites

<b>Sample</b>	<b>E (GPa)</b>	<b>Sample</b>	<b>E (GPa)</b>
<b>ABS-Blank</b>	3.42 ( $\pm 0.2$ )	<b>ABS-10-174</b>	2.77 ( $\pm 0.3$ )
<b>ABS-2</b>	3.59 ( $\pm 0.2$ )	<b>ABS-2-186</b>	3.55 ( $\pm 0.2$ )
<b>ABS-5</b>	3.75 ( $\pm 0.2$ )	<b>ABS-5-186</b>	3.59 ( $\pm 0.4$ )
<b>ABS-10</b>	3.82 ( $\pm 0.1$ )	<b>ABS-10-186</b>	3.43 ( $\pm 0.6$ )
<b>ABS-20</b>	3.50 ( $\pm 0.0$ )	<b>ABS-2-189</b>	3.72 ( $\pm 0.2$ )
<b>ABS-2-174</b>	3.92 ( $\pm 0.2$ )	<b>ABS-5-189</b>	3.81 ( $\pm 0.2$ )
<b>ABS-5-174</b>	3.65 ( $\pm 0.2$ )	<b>ABS-10-189</b>	3.62 ( $\pm 0.1$ )

**Table A. 3** Impact Strength Values for Composites (The composites which are not included in this table were not broken)

<b>Sample</b>	<b>Energy Absorbed (kJ/m<sup>2</sup>)</b>	<b>Sample</b>	<b>Energy Absorbed (kJ/m<sup>2</sup>)</b>
<b>ABS-5</b>	27.7 ( $\pm 2.9$ )	<b>ABS-5-186</b>	18.2 ( $\pm 1.6$ )
<b>ABS-10</b>	18.0 ( $\pm 1.8$ )	<b>ABS-10-186</b>	18.2 ( $\pm 1.5$ )
<b>ABS-20</b>	5.1 ( $\pm 1.3$ )	<b>ABS-5-189</b>	36.8 ( $\pm 3.2$ )
<b>ABS-5-174</b>	22.5 ( $\pm 1.3$ )	<b>ABS-10-189</b>	22.3( $\pm 4.0$ )
<b>ABS-10-174</b>	14.7 ( $\pm 2.4$ )		

## APPENDIX B

### DSC THERMOGRAMS

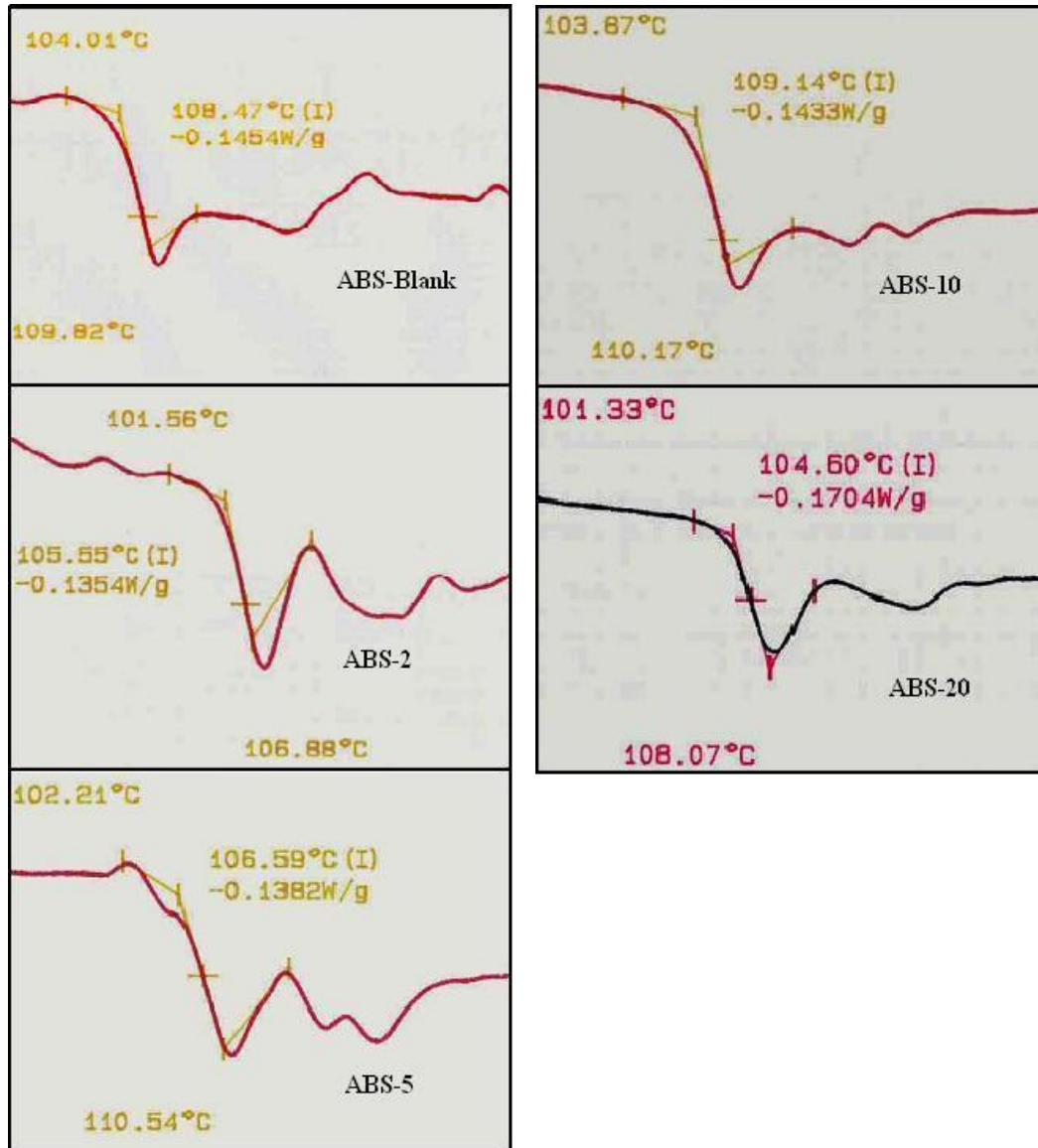


**Figure B. 1** DSC Thermograms of ABS-Blank, ABS-2, ABS-5, ABS-10 and ABS-20

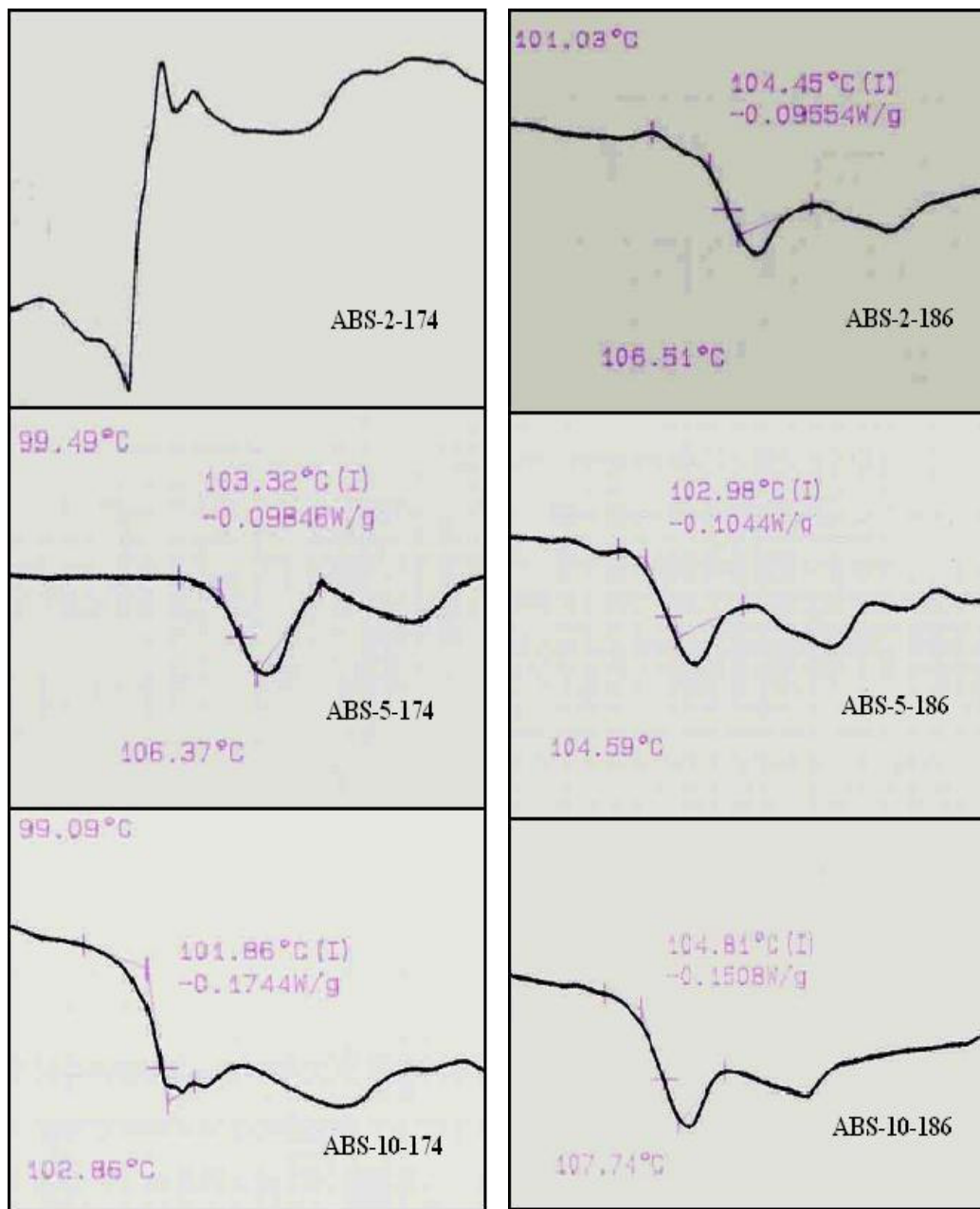


**Figure B. 2** DSC Thermograms of ABS-2-174, ABS-5-174, ABS-10-174, ABS-2-186, ABS-5-186, ABS-10-186

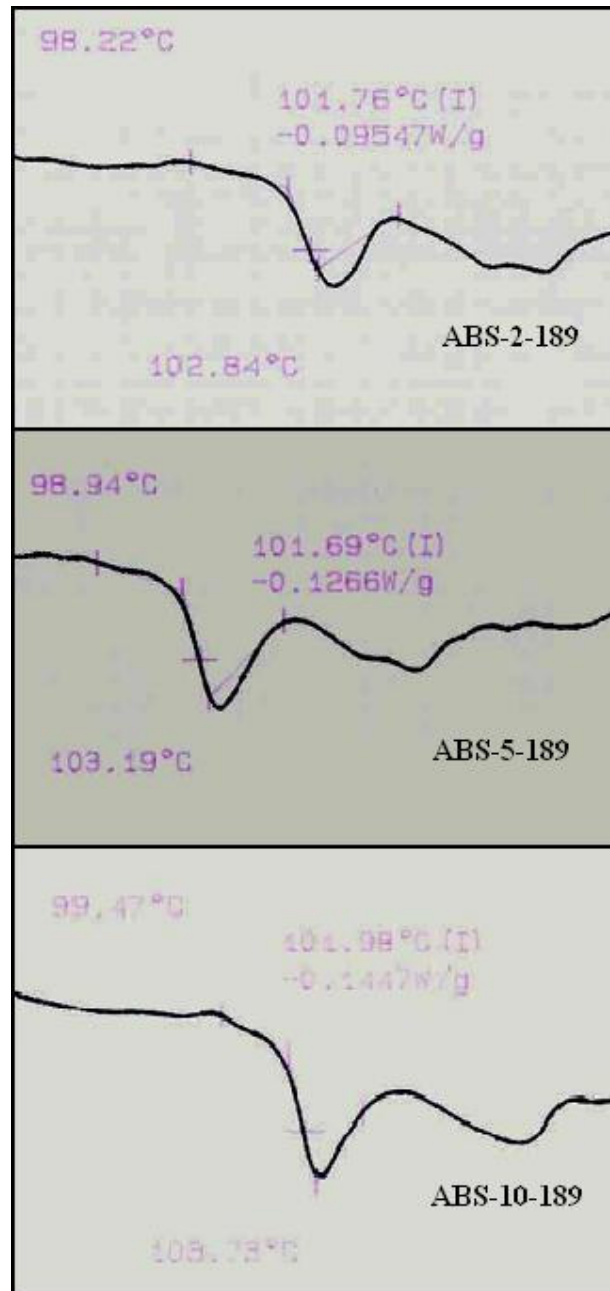


**Figure B. 3** DSC Thermograms of ABS-2-189, ABS-5-189 and ABS-10-189